Global Biogeochemical Cycles

RESEARCH ARTICLE
10.1029/2025GB008545

Special Collection:
Exploring Carbon Cycling in Aquatic Ecosystems Using Novel Analytical and Data-Driven Approaches

Long-Term and Seasonal Drivers of Organic Matter in the Clearwater Tapajós River and Implications for the Amazon River Basin

Martin R. Kurek[1,2], Rafael Muniz[3], José M. S. Moura[4], Bernhard Peucker-Ehrenbrink[5], Robert M. Holmes[6], Amy M. McKenna[7,8], and Robert G. M. Spencer[1,2]

[1]Department of Earth, Ocean and Atmospheric Science, Florida State University, Tallahassee, FL, USA, [2]National High Magnetic Field Laboratory Geochemistry Group, Tallahassee, FL, USA, [3]Doctoral Graduate Program in Society, Nature and Development, Institute of Biodiversity and Forestry, Federal University of Western Pará, Santarém, Brazil, [4]Applied Ecology Laboratory, Interdisciplinary and Intercultural Training Institute, Federal University of Western Pará, Santarém, Brazil, [5]Marine Chemistry and Geochemistry Department, Woods Hole Oceanographic Institution, Woods Hole, MA, USA, [6]Woodwell Climate Research Center, Falmouth, MA, USA, [7]National High Magnetic Field Laboratory Ion Cyclotron Resonance Facility, Tallahassee, FL, USA, [8]Department of Soil & Crop Sciences, Colorado State University, Fort Collins, CO, USA

Key Points:

- Tapajós River dissolved organic matter composition and export is driven both by discharge and seasonal evaporative drying
- Organic carbon fluxes and composition vary interannually due to regional climate events and land use change in the Tapajós basin
- The Tapajós River exports 1.38 Tg of dissolved organic carbon annually to the Amazon mixing zone, similar to the Yukon River carbon flux

Supporting Information:

Supporting Information may be found in the online version of this article.

Correspondence to:
M. R. Kurek,
mkurek@fsu.edu

Citation:
Kurek, M. R., Muniz, R., Moura, J. M. S., Peucker-Ehrenbrink, B., Holmes, R. M., McKenna, A. M., & Spencer, R. G. M. (2025). Long-term and seasonal drivers of organic matter in the clearwater Tapajós River and implications for the Amazon River basin. *Global Biogeochemical Cycles*, *39*, e2025GB008545. https://doi.org/10.1029/2025GB008545

Received 19 FEB 2025
Accepted 8 JUN 2025

Abstract The Amazon River exports over 10% of the global riverine dissolved organic carbon (DOC) flux to the ocean. However, several downstream clearwater tributaries, such as the Tapajós River, are typically not included in these measurements, omitting a crucial part of the Amazon carbon cycle. This study investigated near-monthly DOC and dissolved organic matter (DOM) composition via optical, fluorescence spectroscopy, and ultra-high resolution mass spectrometry (FT-ICR MS) of the Tapajós River for 8 years (2016–2024) to better understand patterns and drivers of potential organic carbon export to the lower Amazon River. DOM composition and DOC export were driven by the seasonal flood pulse of the Tapajós River, exporting aromatic terrestrial DOM from the watershed during high discharge and internally produced algal or microbial DOM during dry periods. On average, we report that the Tapajós River exports 1.38 Tg DOC annually to the downstream Amazon mixing zone, representing an amount of DOC exported by other major world rivers such as the Yukon or Mekong River. Furthermore, organic carbon export varied interannually with less DOC exported during dry El Niño events and more algal-derived DOM exported during bloom periods. Finally, as grassland and cropland landcover increased over the study period, we observed an average decrease in aromatic DOM and an increase in microbially processed fluorophores. Our study suggests that temperature, precipitation, and anthropogenic land use changes in clearwater rivers will impact carbon export across the lower Amazon River network.

Plain Language Summary The Amazon is the largest river in the world, delivering over 20% of the global riverine discharge and 10% of dissolved organic carbon (DOC) to the ocean. The Tapajós River is a major clearwater tributary of the Amazon that is often omitted from the total Amazon River delivery to the ocean due its downstream location from historical sampling sites; however, its role in the Amazon carbon cycle remains important. We sampled the Tapajós River over 8 years and determined that patterns of organic matter delivery to the Amazon River are highly seasonal. More organic carbon is exported from the landscape during high discharge periods, whereas the landscape is disconnected during dry periods. The Tapajós River potentially adds an additional 5% of DOC to what is exported from the Amazon River each year, an amount comparable to other world rivers such as the Yukon or Mekong River, but this export is highly dependent on regional climate with less carbon exported during dry years. Finally, as land was converted to grasslands and cropland in the Tapajós basin, the river exported more microbially altered organic matter, which will likely impact carbon reactivity in the downstream Amazon River.

1. Introduction

River systems are highly complex and dynamic networks responsible for both carbon transport, processing, and production. Globally, rivers transport between 235 and 250 Tg of dissolved organic carbon (DOC) from terrestrial systems to the ocean each year (Hedges et al., 1997; M. Li et al., 2019; Spencer & Raymond, 2024) and outgas between 1.8 and 2.9 Pg C yr^{-1} as CO_2 to the atmosphere (Battin et al., 2023; Raymond et al., 2013; Sawakuchi

et al., 2017). Thus, river systems serve as the nexus between pools of terrestrial, aquatic, and atmospheric carbon with DOC as a highly mobile and important intermediary (Aufdenkampe et al., 2011; Battin et al., 2009; Cole et al., 2007; Drake et al., 2018). DOC represents the quantified portion of dissolved organic matter (DOM) which incorporates carbon from a variety of terrestrial and internal (autochthonous) sources and serves many ecosystem functions, namely as a reduced carbon source for aquatic respiration (Amon & Benner, 1996; Battin et al., 2009; Mayorga et al., 2005). The composition of DOM mixtures can therefore be used to infer the origin, processing history, and lability of organic matter exported from river systems via biological and photodegradation (Berggren et al., 2022; Kellerman et al., 2018; Riedel et al., 2016; Ward et al., 2013). While studies have proposed varying mechanisms that govern DOM availability and processing throughout the reaches of a river network and its floodplain, they are all highly dependent on river discharge and hydrologic connectivity to the landscape (Amon & Benner, 1996; Creed et al., 2015; Raymond et al., 2016; Vannote et al., 1980). As global air temperatures continue to increase and precipitation becomes more variable, riverine hydrology and flow paths will likely be impacted (Gudmundsson et al., 2021; Van Vliet et al., 2013; Wu et al., 2023), making it important to understand the controls on carbon sourcing and export from the landscape. This is particularly true for tropical systems such as the Amazon River, which has experienced a recent amplification in hydroclimate and an increase in annual DOC export (Gloor et al., 2013; M. Li et al., 2019; Liang et al., 2020).

The Amazon River is the largest river on Earth by discharge and watershed area. The river delivers nearly 20% of the global riverine discharge to the ocean (5,346–5,849 km^3 yr^{-1}) integrated across over 6 million square kilometers (Drake et al., 2021; Hastie et al., 2019; Kurek et al., 2021). Discharge and solute export are controlled by the "rhythm" of the Amazon flood pulse, whereby heavy rainfall across the basin increases surface runoff resulting in a prominent yearly discharge peak with a sinusoidal pattern (Marengo, 2006; Richey et al., 1989; Sioli, 1984). During high discharge, biogenic solutes, such as DOC and DOM, are flushed from the landscape and mobilized into the river, thereby increasing their concentration and the relative contribution of terrestrial organic matter to the overall composition (Devol et al., 1995; Drake et al., 2021; McClain et al., 1997; Richey et al., 1990). Conversely, flushing is reduced during low discharge and the river exports relatively less terrestrial DOM but incorporates DOM from other sources in the floodplain (Bustillo et al., 2011; Quay et al., 1992; Ward et al., 2015). DOM is respired and processed during transport along the Amazon River network and through the offshore Amazon plume (Aufdenkampe et al., 2007; Kurek et al., 2022; Medeiros et al., 2015; Seidel et al., 2015; Ward et al., 2013) with ultimately over 10% of global riverine DOC to the ocean exported every year (25.5–26.9 Tg C yr^{-1}) from the furthest downstream gauging station at Óbidos, Brazil (Kurek et al., 2021; Richey et al., 1990; Spencer & Raymond, 2024). Although nearly 90% of the discharge and DOC flux of the mainstem to the Atlantic Ocean is captured at Óbidos (Coynel et al., 2005; Moreira-Turcq et al., 2003; Spencer & Raymond, 2024), the station remains upstream of major clearwater tributaries, the Tocantins, Xingu, and Tapajós River, whose inputs into the Amazon plume and Atlantic Ocean are typically not accounted for. Despite their comparatively limited contribution to the total Amazon River flux, these rivers are sizeable compared to other major global river systems and are important sinks for sedimentary organic carbon (Bertassoli et al., 2017; Rosengard et al., 2024) and sources of atmospheric CO_2 and CH_4 (Sawakuchi et al., 2014, 2017). These rivers also deliver biolabile DOM sourced from algae and macrophytes to the Amazon River (Doherty et al., 2017; Seidel et al., 2016; Ward et al., 2015), potentially enhancing the mineralization of Amazon River DOM at their confluence (Ward et al., 2016).

Of all the clearwater rivers, the Tapajós River has a greater average discharge and is typically considered to export more DOC (Moreira-Turcq et al., 2003; Spencer & Raymond, 2024). However, flux estimates have relied on limited monthly sampling over only a few years and given the large variations in discharge between wet and dry seasons (Moreira-Turcq et al., 2003; Ward et al., 2015), actual monthly and annual fluxes may differ. Limited sampling may also make it difficult to assess the effects of climate anomalies, such as droughts or flooding, on Tapajós River export. Such climate anomalies due to El Niño Southern Oscillation can impact both the magnitude and composition of exported DOM from subtropical-tropical rivers including the Amazon (e.g., Kurek et al., 2021; Qu et al., 2020), making it likely for annual fluxes to differ considerably. Furthermore, previous work has provided valuable comparisons of Tapajós River DOM to other Amazon River systems, but these measurements have also been limited to discrete monthly sampling over only a couple of years (Albéric et al., 2018; Seidel et al., 2016; Ward et al., 2015). Monthly samples have primarily been assessed near the Tapajós-Amazon confluence (Santarém, Figure 1), which can be subject to strong backwater effects from the Amazon River and mixing of the blackwater Arapiuns River, making it difficult to fully characterize DOM sourced from the Tapajós River watershed (S. Li, Harir, Schmitt-Kopplin, Gonsior, et al., 2023; S. Li, Harir, Schmitt-Kopplin, Machado-

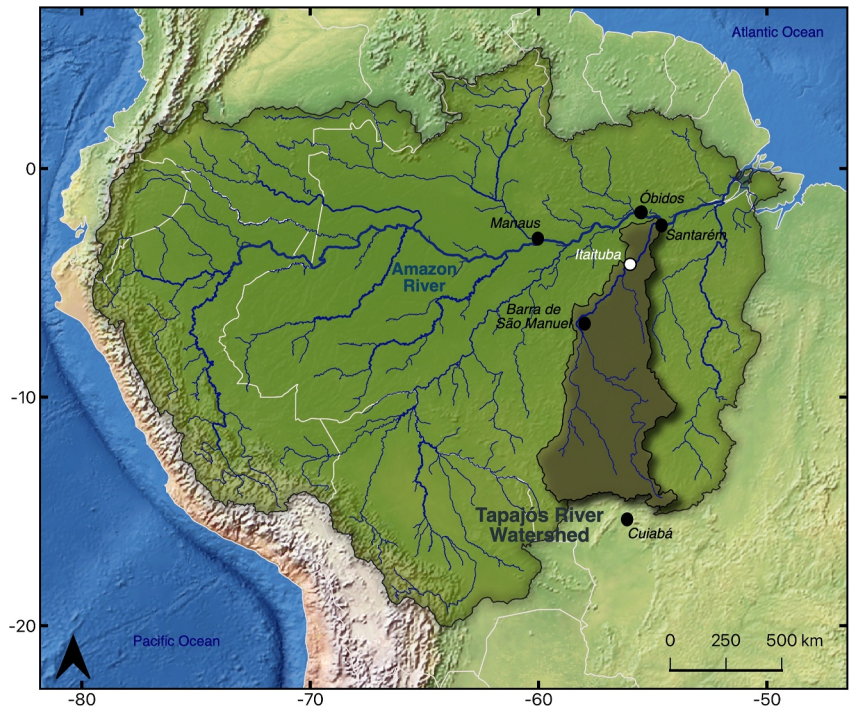

Figure 1. Amazon River basin (highlighted region) with The Tapajós River watershed (shaded region) and sampling site on the Tapajós River (Itaituba, white point).

Silva, et al., 2023; Seidel et al., 2016; Ward et al., 2015). Finally, the Tapajós River watershed is experiencing profound changes to its landscape through extensive damming, expansion of gold mining operations, deforestation, and commodity-driven land conversion, all of which have impacted the ecology and biogeochemistry of the river (Farella et al., 2001; Farinosi et al., 2019; Lobo et al., 2016; Nóbrega, Guzha, et al., 2018). Coupled with projected increases in air temperatures and changes in regional precipitation, these impacts will likely affect hydrology and downstream carbon cycling across the Tapajós mainstem to the lower reaches of the Amazon River. To date, no study has investigated the long-term export of DOC and DOM from the Tapajós River, or other major Amazonian tributaries, as influenced by changes in climate and land use.

This study integrates DOC measurements, optical properties including chromophoric DOM (CDOM), and fluorescence components with hydrological and climate properties to investigate the sources and drivers of DOM composition in the Tapajós River. Similar techniques have been employed across other tropical rivers and demonstrated their utility in relating DOM composition to regional carbon cycling (e.g., Dalmagro et al., 2017; Gonsior et al., 2016; Lambert et al., 2016; Mann et al., 2014). Additionally, we utilized molecular-level analysis via 21 T Fourier transform-ion cyclotron resonance mass spectrometry (FT-ICR MS), enabling the resolution of mass differences that are <1 mDa apart (Hendrickson et al., 2015; Smith et al., 2018). Such measurements have revealed additional patterns in the average DOM oxidation state, stability, and quantitative relationships with organic N and S (Boye et al., 2017; Kellerman et al., 2018; Kurek et al., 2020; Poulin et al., 2017; Riedel et al., 2016). Coupling these measurements with bulk concentrations and optical data provides a comprehensive analysis of various DOM pools in the Tapajós River and allows for more comparisons to and inclusion of other DOM studies that utilize various methodologies, particularly across the Global South. We present an 8-year near-monthly characterization of Tapajós River hydrology, DOC, and properties as a comparison to other Amazonian rivers. Our work also includes refined estimates of discharge, DOC, and CDOM fluxes as well as an analysis of changing landcover effects on DOM exported from the Tapajós River and similar clearwater tributaries.

2. Materials and Methods

2.1. Study Site and Field Sampling

The Tapajós River is the fifth largest river basin that drains into the Amazon River, spanning nearly 500,000 km^2 in north-central Brazil (Figure 1). The headwaters originate in the state of Mato Grosso just north of Cuiabá, Brazil as the Juruena River and Teles Pires River, which flow northward and confluence at Barra de São Manuel, dropping from nearly 800 to 100 m in elevation. At this point, the rivers form the Tapajós River, which continues northward through the state of Pará, Brazil as the elevation drops to just a few meters above sea level. North of Itaituba, the river water velocity decreases and the channel widens, forming a massive lake (ria) prior to its confluence with the Amazon River near Santarém (Bertassoli et al., 2017).

Tapajós is a clearwater river with low dissolved and suspended solids, as well as a slightly alkaline pH draining the Precambrian bedrock of the Brazilian Shield (Moquet et al., 2016; Ríos-Villamizar et al., 2020; Sioli, 1984). The basin experiences an overall humid tropical climate and is heavily forested, particularly in the north, which is dominated by tropical evergreen rainforests that are largely protected in the states of Pará and Amazonas. The southern portions are covered by Cerrado savanna with areas in the State of Mato Grosso experiencing heavy deforestation, land conversion to pastures, damming, and small-scale gold mines along many tributaries (Castello & Macedo, 2016; Farinosi et al., 2019; Lobo et al., 2016; Pavanato et al., 2016). Details regarding landcover data are provided (Text S1 in Supporting Information S1). The watershed is on average 62% forest, 15% savanna, 15% grassland, and 8% cropland from 2016 to 2022 (Friedl & Sulla-Menashe, 2019).

Water samples were collected near-monthly from the Tapajós River from 28 January 2016 to 30 November 2023, upstream of Itaituba (4°20′15.0″S, 56°04′10.3″W; Figure 1). Three water samples (1 L) were collected at 0.5 m depth from the river across the channel in equal spacing and combined into a 4 L acid-washed carboy to make a composite sample. The water was filtered through a 0.45 μm capsule filter with a peristaltic pump into acid-rinsed high-density polyethylene (HDPE) bottles. Filtered samples were kept cold during transport and immediately frozen upon transfer to the laboratory and kept in the dark until analysis. Samples for water isotope analysis (δ^{18}O, δ^{2}H) were collected in 30 mL HDPE bottles that were filled to capacity, free of air, and stored in a dark, cool place prior to analysis. In situ water temperature, dissolved oxygen (DO), specific conductivity (SpC), and pH were measured in the center of the river channel at 0.5 m depth with a calibrated YSI Professional Plus multimeter.

2.2. Discharge, Climate, and Water Isotope Analysis

Near-daily discharge measurements (Q, m^3 s^{-1}) from the Tapajós River between 2015 and 2024 were obtained from the closest gauging station to Itaituba located 60 km upstream at Buburé (4°36′56.2″S, 56°19′30.0″W) via the Brazilian National Water Agency (https://www.snirh.gov.br/hidroweb/serieshistoricas). When discharge was not available at Buburé, missing values were interpolated from measurements taken at the Barra de São Manuel gauging station (7°20′22.9″S, 58°09′19.1″W) using a linear fit of 4 days lagged values based on the travel time of water across the two stations (Text S1; Figures S1 and S2 in Supporting Information S1). Daily accumulated precipitation values at 0.1° resolution were obtained from the NASA Global Precipitation Monitoring v6.0 data archive (Huffman et al., 2019) and daily 2-m mean air temperatures at 0.5 × 0.625° resolution were obtained from the NASA Modern-Era Retrospective analysis for Research and Applications version 2 (MERRA-2) data archive (Gelaro et al., 2017). Both daily precipitation and temperature values were averaged over the Tapajós River basin area.

Stable isotopes of the water molecule (δ^{18}O, δ^{2}H) from river water samples were analyzed at the Isotope Hydrology Laboratory of the International Atomic Energy Agency (IAEA, Vienna, Austria) through the Global Network of Isotopes in Rivers (GNIR). For samples up to sampling dates of August 2017, analyses were conducted in replicate by Off-Axis Integrated Cavity Output Spectroscopy (OA-ICOS, TLWIA 45EP, Los Gatos Inc., USA) with nine injections per sample vial of which five were accepted. The later batch was analyzed, again in replicate, via dual-isotope Cavity Ringdown Spectroscopy (CRDS, 2130i/2140i, Picarro Inc., USA) with six injections per vial (three accepted). Data post-processing included amount-linearity correction for OA-ICOS data, memory correction and normalization to the VSMOW-SLAP scale using LIMS for Lasers 2015 (Coplen & Wassenaar, 2015). The analytical uncertainty for δ^{18}O and δ^{2}H was better than ±0.15 and ±0.7‰ for the OA-ICOS measurements, and better than ±0.1 and ±0.5‰ for those via CRDS. Data for Amazon River rainwater

($\delta^{18}O$, $\delta^{2}H$) were obtained from the IAEA Water Isotope System for Electronic Retrieval (WISER, 2022; https://nucleus.iaea.org/wiser).

2.3. DOC Analysis

Filtered Tapajós River water samples were acidified (HCl, pH 2) and DOC concentrations were measured with a Shimadzu TOC-L CPH high temperature catalytic oxidation total organic carbon analyzer (Shimadzu Corp., Kyoto, Japan). Samples were sparged with air for 8 min and DOC was quantified using a five-point calibration curve according to an established methodology (e.g., Kurek et al., 2024).

2.4. Optical and Fluorescence Spectroscopy

UV-visible absorbance spectra were measured at room temperature in a 1-cm quartz cuvette with a Horiba Scientific Aqualog (Horiba Ltd., Kyoto, Japan) at wavelengths of 230–800 nm. CDOM was determined as the Napierian absorption coefficient at 350 nm (a_{350}; m^{-1}). Spectral slopes, as related to aromaticity and molecular weight, were calculated from 275 to 295 ($S_{275–295}$; nm^{-1}) and 350–400 nm ($S_{350–400}$; nm^{-1}; Helms et al., 2008). Specific UV absorbance at 254 nm ($SUVA_{254}$; L mg C^{-1} m^{-1}) indicates the CDOM content of DOC and was calculated by dividing the decadic absorption coefficient at 254 nm by the DOC concentration (Weishaar et al., 2003).

Excitation-Emission matrices (EEMs) from fluorescence spectra were measured at room temperature in a 1-cm quartz cuvette using a Horiba Scientific Aqualog (Horiba Ltd., Kyoto, Japan). EEMs were collected at 250–500 nm excitation wavelengths and 300–600 nm emission wavelengths with 5 and 2 nm intervals, respectively, at integration times ranging from 3 to 6s. EEMs were corrected for lamp intensity (Cory et al., 2010) and inner filter effects (Kothawala et al., 2013), and normalized to Raman units (Stedmon et al., 2003). Parallel factor analysis (PARAFAC) was modeled with 81 individual EEMs and validated using core consistency diagnostics and split-half validation (Murphy et al., 2013), yielding a 5-component model that explained 99.93% of the variance. The model was compared to previously identified components using an online library (www.openfluor.org; Murphy et al., 2013). Finally, the fluorescence index (FI), which describes terrestrial and microbial contributions to DOM composition, was calculated from the emission intensity at 470 and 520 nm at excitation 370 nm (Cory & McKnight, 2005; McKnight et al., 2001).

2.5. Solid Phase Extraction (SPE) and FT-ICR MS Analysis

Filtered water samples were acidified (HCl, pH 2) and extracted using Bond-Elut PPL columns (Agilent Technologies Inc., Santa Clara, CA) following an established methodology (Dittmar et al., 2008). Columns were soaked with methanol overnight (conditioned), rinsed with methanol, and rinsed twice with acidified Milli-Q water (HCl, pH 2). Approximately 50 μg C was isolated onto 100 mg 3 mL bed volume PPL columns (assuming at least 50% recovery), eluted with 1 mL methanol into precombusted (550°C, >4 hr) glass vials, and stored at −20°C until analysis. DOC recovery was assessed on several samples with duplicate extractions. Methanol extracts were collected in 40 mL glass vials and evaporated by gently drying (50°C, overnight). The remaining residue was redissolved in Milli-Q water (HCl, pH 2) and the DOC concentrations were measured using methods described in Section 2.3 (e.g., Kurek et al., 2024).

Methanolic extracts were analyzed on a custom-built hybrid linear ion trap ultra-high resolution FT-ICR mass spectrometer equipped with a 21T superconducting solenoid magnet at the National High Magnetic Field Laboratory (Tallahassee, FL; Hendrickson et al., 2015; Smith et al., 2018). Negatively charged ions from DOM were produced via electrospray ionization (ESI) at a flow rate of 500 nL min^{-1} via a syringe pump. Typical conditions for ion formation included: emitter voltage, −2.8–3.2 kV; S-lens RF level, 40%; and heated metal capillary temperature, 350°C. The resulting spectra were conditionally co-added to yield 75 individual time domain transients of 3.1 s for each experiment. Co-added mass spectra were phase-corrected (Xian et al., 2010) and peaks were internally calibrated based on 10–15 highly abundant O-containing series using a "walking" calibration (Savory et al., 2011) as described previously (e.g., Kurek et al., 2024). Further details regarding FT-ICR MS methodology are provided (Text S1 in Supporting Information S1).

2.6. FT-ICR MS Post-Processing

Mass spectral peaks (>6σ root-mean-square (RMS) baseline noise) were exported to a peak list and processed using PetroOrg© (Corilo, 2014). Molecular formulae were assigned to ions constrained by $C_{4\text{-}75}H_{4\text{-}150}O_{1\text{-}30}N_{0\text{-}4}S_{0\text{-}2}$ not exceeding 300 ppb error (e.g., Kurek et al., 2024). For all spectra, between 15,000 and 22,000 species were assigned elemental compositions (mean: 18,000) with RMS error between 46 and 78 ppb (mean: 61) and achieved resolving power >1,600,000 at *m/z* 400. Molecular formula properties, including the modified aromaticity index (AI_{mod}) and nominal carbon oxidation state (NOSC), were calculated according to Koch and Dittmar (2006, 2016) and Boye et al. (2017), respectively. Mass-weighted stoichiometric ratios were averaged (H/C, O/C, N/C, S/C) and formulae were also grouped into broad compound classes based on the percent relative abundance of their heteroatom classes (CHO, CHON, CHOS, and CHONS). Molecular formulae were grouped into compounds based on Šantl-Temkiv et al. (2013) including condensed aromatics (CA; $0.67 < AI_{mod}$), polyphenolics (PPh; $0.50 < AI_{mod} < 0.67$), highly unsaturated and phenolic low O/C ($HUP_{Low\ O/C}$; $AI_{mod} < 0.50$, $H/C < 1.5$, $O/C < 0.5$), HUP high O/C ($HUP_{High\ O/C}$; $AI_{mod} < 0.50$, $H/C < 1.5$, $0.5 \leq O/C$), and aliphatic (Ali; $1.5 \leq H/C$), and the percent relative abundance of each class was summed. Molecular formulae belonging to the island of stability (IOS), a group of 361 individual molecular formulae first reported by Lechtenfeld et al. (2014) in marine DOM, were identified in each individual mass spectrum. Their relative abundances were summed to estimate the percent relative abundance of IOS molecular formulae in each river sample as an indicator of stable, aged DOM (Kellerman et al., 2018). Data derived from individual mass spectra including number of peak assignments, RMS error, and calculated properties for all species identified by 21T FT-ICR MS used in this publication are provided in Data Set S1.

2.7. Data Analysis

Data analysis including linear regression was performed in R (R Core Team, 2020) and visualized using the ggplot2 package (Wickham, 2016). Spearman correlations between the yearly mean of each DOM parameter and yearly landcover proportion between 2016 and 2022 were calculated using the psych package in R (Revelle, 2024). Spearman correlations between the relative abundance of all common molecular formulae and climate/hydrological variables were also conducted using a similar methodology in R. Significantly correlated molecular formulae were only considered if they had a false discovery rate corrected *p*-value ($p < 0.05$; Benjamini & Hochberg, 1995). PARAFAC modeling was conducted in MATLAB using packages from Murphy et al. (2013). Relationships between DOC, CDOM concentration and discharge were fit using a power law equation:

$$C = a \times Q^b$$

Where C is the concentration of DOC or CDOM, Q is the river water discharge, and a and b are fitted constants. Positive values of b suggest mobilization into the river, negative values suggest dilution, and zero or near-zero values indicate chemostasis as has been described for many *C-Q* relationships (Drake et al., 2021; Musolff et al., 2015; Rose et al., 2018).

2.8. Flux Estimates

Daily discharge, DOC (kg day^{-1}), and CDOM absorbance at 350 nm (m^2 day^{-1}) fluxes were modeled using instantaneous discharge measurements and concentrations with the FORTRAN Load Estimator (LOADEST) program (Runkel et al., 2004). Resulting daily fluxes were summed to yield annual fluxes across 2016–2024. The calibration equation was derived using the Adjusted Maximum Likelihood Estimator (AMLE) and the regression model number was set to default (MODNO = 0), allowing for selection of the best model based on Akaike Information Criteria. The validity of the model was verified from the output of the r^2 of the AMLE, residuals data, and the serial correlation of residuals, including confirmation that the residuals were normally distributed according to previous methods (Dornblaser & Striegl, 2009).

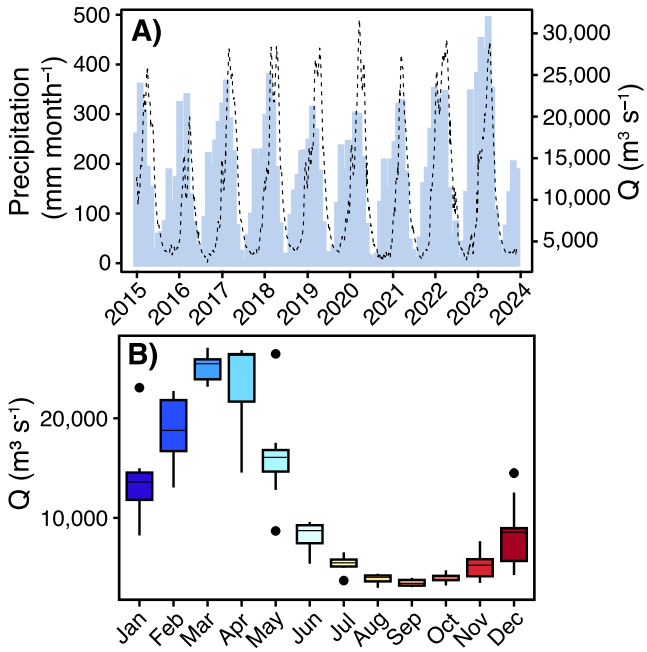

Figure 2. (a) Daily discharge (Q) values of the Tapajós River at Itaituba (dotted line) with monthly accumulated precipitation (blue shaded region) averaged across the Tapajós River basin during 2015–2023. (b) Boxplot of average Tapajós River discharge (Q) by a month.

3. Results

3.1. Hydrologic Setting and Water Isotopes

Tapajós River water was collected and analyzed from 2016 to the end of 2023; however, temperature, precipitation, and discharge measurements are presented for context from the beginning of 2015 due to the lag time between peak precipitation and discharge in Amazonian rivers (e.g., Drake et al., 2021). Mean annual precipitation across the Tapajós River basin ranged from 1,802 to 2,798 mm (mean: 2,142 mm) while mean annual air temperatures ranged from 25.4 to 27.2°C (mean: 26.3°C; Table S1 in Supporting Information S1). Maximum precipitation occurred between February-March (329 mm $month^{-1}$) and minimum precipitation occurred in July (14 mm $month^{-1}$; Figure S3a in Supporting Information S1). Similarly, average air temperatures peaked in September (29.6°C) while minimum air temperatures were between January-June (25.0°C; Figure S3b in Supporting Information S1). Annual precipitation in the Tapajós basin was similar to other clearwater rivers such as the Trombetas (1,822; Moreira-Turcq et al., 2003) and Xingu (2,048 mm; Panday et al., 2015) but lower than the Tocantins (2,743 mm; Neu et al., 2023).

Mean annual Tapajós River discharge ranged from 7,751 to 12,871 $m^3\ s^{-1}$ (mean: 11,067 $m^3\ s^{-1}$; Table S1 in Supporting Information S1) with some inter-annual variability over the study period (Figure 2a). Discharge peaked between March and April (27,550 $m^3\ s^{-1}$; Figure 2b) with the annual maximum ranging from 19,983 to 31,674 $m^3\ s^{-1}$ (Table S1 in Supporting Information S1). Minimum discharge occurred in September (3,183 $m^3\ s^{-1}$; Figure 2b) and ranged between 2,503 and 3,788 $m^3\ s^{-1}$ annually (Table S1 in Supporting Information S1). Monthly average discharge was comparable to findings from 1994 to 1998 (2,630–22,470 $m^3\ s^{-1}$; Moreira-Turcq et al., 2003) but greater than other clearwater rivers such as the Trombetas (2,555 $m^3\ s^{-1}$; Moreira-Turcq et al., 2003), Xingu (7,806 $m^3\ s^{-1}$; Panday et al., 2015), and the Tocantins (10,800 $m^3\ s^{-1}$; Neu et al., 2023).

Precipitation and specific discharge (Q normalized to basin area) correlated positively; however, there was a considerable 3 to 4-month lag between the onset of increased precipitation and the rising limb of the hydrograph, resulting in a counterclockwise hysteresis pattern (Figures 2a and 3a). Furthermore, precipitation was on average 4.2 times greater than specific discharge (below the 1:1 line) except from June-July during the falling limb, when monthly discharge and precipitation were approximately equal (around the 1:1 line; Figure 3a).

Mean water isotope ratios ($\delta^{18}O$ and $\delta^{2}H$) from the Tapajós River were −4.9‰ and −30.7‰, respectively, and ranged between −6.6 and −4.0‰ ($\delta^{18}O$) and −42.5 to −23.5‰ ($\delta^{2}H$). All values were within ranges previously reported for Amazon River water at Óbidos (Drake et al., 2021; Mortatti et al., 1997) and mean $\delta^{18}O$ values were similar to Tapajós River water samples measured at Jacareacanga, Brazil, nearly 290 km south of Itaituba (mean: −4.9‰, −6.0% to −4.0%; Salati et al., 1979). The linear regression between Tapajós River $\delta^{18}O$ and $\delta^{2}H$ yielded an overall slope of 6.5 and intercept of 1.5 (Figure 3b). This slope was shallower than the slope of the Brazil Local Meteoric Water Line (8.6; Drake et al., 2021), precipitation from Santarém, Brazil at the northern edge of the basin (8.4; Figure 3b, black dotted line), and precipitation from Cuiabá, Brazil, south of Tapajós River headwaters (7.5; Figure 3b, red dotted line; WISER, 2022). Both water isotopes were negatively correlated with discharge having a prominent clockwise hysteresis pattern, particularly from July-October (Figures 3c and 3d). Finally, deuterium excess (D-excess) also varied by months (Figure S3c in Supporting Information S1). The average D-excess was 8.9‰ which is lower than the D-excess of precipitation from Cuiabá (9.8‰; WISER, 2022), Jacareacanga (10.0‰; Salati et al., 1979), Santarém (12.0–15.5‰; Martinelli et al., 1996; WISER, 2022), and Amazon River water (13.6‰; Drake et al., 2021).

3.2. Water Quality Parameters

SpC ranged from 13.0 to 26.0 μS cm^{-1} (mean: 16.8 μS cm^{-1}) and was slightly lower in March than the rest of the year (Figure S4a in Supporting Information S1). pH ranged from 6.2 to 7.8 (mean: 7.0) with lower values between

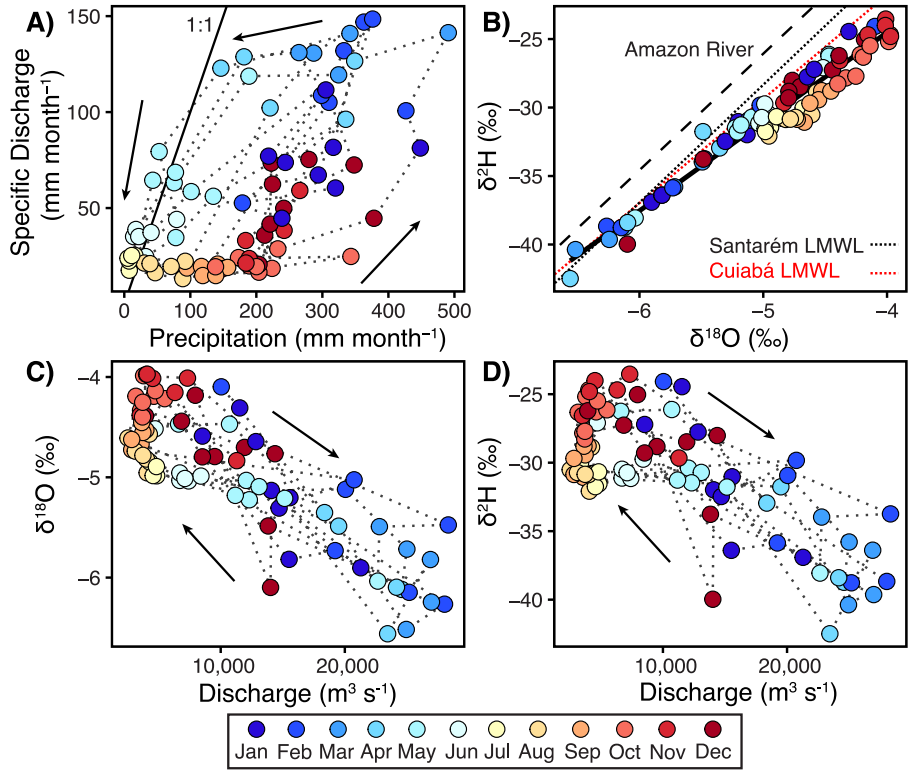

Figure 3. (a) Monthly specific discharge (discharge/watershed area) with monthly precipitation. (b) Stable isotope ratios of water ($\delta^{18}O$ vs. $\delta^{2}H$) with linear regression (solid black line). Amazon River water trend (black long dashed line; Drake et al., 2021), the Local Meteoric Water Line (LMWL) from Santarém (black short dashed line; WISER, 2022), and LMWL from Cuiabá (red short dashed line; WISER, 2022) are plotted for reference. (c) $\delta^{18}O$ with monthly discharge and (d) $\delta^{2}H$ with monthly discharge. Points are colored according to sampling month and arrows indicate direction of hysteresis (clockwise vs. counterclockwise).

February and March (Figure S4b in Supporting Information S1). DO concentrations were between 4.5 and 8.4 mg L^{-1} (mean: 6.6 mg L^{-1}) and did not follow a discernible seasonal pattern (Figure S4c in Supporting Information S1). Finally, water temperatures at Itaituba were generally higher than average air temperatures across the Tapajós basin (26.9–32.8, mean: 29.7°C) but followed the same seasonal pattern (Figure S4d in Supporting Information S1). Water temperature and DO were in similar ranges to previous measurements from the Amazon and Tocantins River (Drake et al., 2021; Neu et al., 2023) while SpC and pH were consistent with many other Amazonian clearwater tributaries (Ríos-Villamizar et al., 2020).

3.3. DOC Concentrations and DOM Optical/Fluorescence Properties

DOC concentrations ranged from 0.9 to 9.2 mg L^{-1} (mean: 3.3 mg L^{-1}; Figure 4a) and were greater than other downstream clearwater tributaries such as the Xingu (2.4 mg L^{-1}; Ward et al., 2016) and Tocantins (2.8 mg L^{-1}; Neu et al., 2023), but lower than the Amazon River (4.2 mg L^{-1}; Drake et al., 2021), the Trombetas (5.3 mg L^{-1}; Moreira-Turcq et al., 2003), and the Rio Negro (7.7–10.6 mg L^{-1}; Gonsior et al., 2016; Simon et al., 2019). CDOM absorption at 350 nm (a_{350}) ranged from 1.3 to 15.9 m^{-1} (mean: 7.2 m^{-1}; Figure 4a) and was lower than the average of the Amazon River (12.2 m^{-1}; Drake et al., 2021). Both DOC and CDOM varied with discharge, where the lowest values occurred during minimum discharge in September, while the largest values occurred on the rising limb of the hydrograph between December-February (Figure 4a). This is also illustrated by the significant positive correlations of DOC and CDOM with discharge ($p < 0.0001$; Figures S5a and S5b in Supporting Information S1). Both relationships displayed positive clockwise hysteresis and were fit with positive b-values (DOC: 0.49, CDOM: 0.74).

$SUVA_{254}$ ranged from 1.9 to 4.7 L mg C^{-1} m^{-1} (mean: 3.4 L mg C^{-1} m^{-1}) and followed the discharge patterns of DOC and CDOM (Figure 4c). In contrast, $S_{275–295}$ (12.1–36.0, mean: 16.0 10^{3} nm^{-1}) and FI (1.41–1.56, mean:

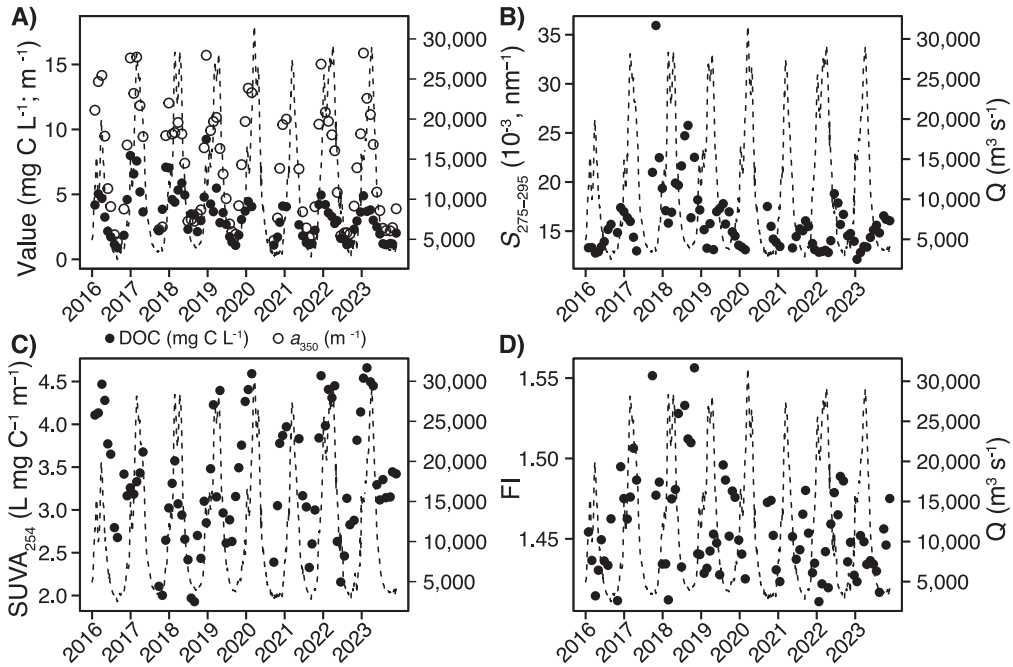

Figure 4. Line plots of: (a) dissolved organic carbon (black points) and CDOM (open circles), (b) $S_{275–295}$, (c) $SUVA_{254}$, and (d) FI measured from Tapajós River water samples during 2016–2023. Discharge (Q) is indicated by the dashed black line.

1.46) followed opposite trends peaking during low discharge and were lowest during the rising limb (Figures 4b and 4d). These trends were comparable to other tropical rivers including Congo River tributaries and the Cuiabá River in Mato Grosso; however, Tapajós River $SUVA_{254}$ was generally lower while average $S_{275–295}$ and FI values were higher (Dalmagro et al., 2017; Mann et al., 2014; Spencer et al., 2010).

3.4. SPE Recovery

SPE-DOM extraction efficiency was assessed across six samples from various months spanning 2016–2024. Mean recovery was 53 ± 18% suggesting that at least half of the extracted DOM was retained on PPL and a large part of the DOM pool could be represented via FT-ICR MS (Yvin et al., 2024). This was slightly lower than values reported from riverine/coastal DOM (62%–65%; Dittmar et al., 2008) and the Amazon River plume (56%–72%; Seidel et al., 2015) but generally higher than groundwater DOM (~40%; Yvin et al., 2024).

3.5. FT-ICR MS DOM Composition

CHO-containing formulae were the most abundant across the study period (67.6–80.2, mean: 75.5%) and were greatest during the rising limb and lowest during minimum discharge (Figure 5a). In contrast, CHON (16.5–28.3, mean: 20.0%), CHOS (2.1–8.0, mean: 3.8%), and CHONS (0.2–1.4, mean: 0.7%) followed the opposite trend (Figure 5a). Compared to the Amazon River and the Rio Negro, Tapajós River DOM is more enriched in N- and S-containing formulae (Kurek et al., 2022; S. Li, Harir, Schmitt-Kopplin, Gonsior, et al., 2023) and follows the seasonal N and S enrichment of what has been observed near the mixing zone at low discharge (Seidel et al., 2016).

Inferred compound classes also followed similar patterns to heteroatoms with important differences (Figure 5b). $HUP_{High\ O/C}$ compounds were the most abundant (32.1–49.2, mean: 41.8%), with the greatest relative abundance during the rising limb and lowest at minimum discharge. $HUP_{Low\ O/C}$ (25.3–36.9, mean: 30.9%) and aliphatics (2.4%–25.5%, mean: 7.2%) followed trends similar to N and S-containing formulae; however, aliphatics with O/C < 0.5 ($Ali_{Low\ O/C}$) peaked 2 months earlier in July (Figure 5b). Furthermore, CA (1.5–8.6, mean: 8.6%) and PPh relative abundance (10.0–24.8, mean 16.7%) were highest during peak discharge, rather than on the rising limb. Compound class proportions were similar to the Amazon River, but the Tapajós had a greater abundance of $HUP_{High\ O/C}$ compounds relative to $HUP_{Low\ O/C}$ (Kurek et al., 2022). Elemental stoichiometry followed

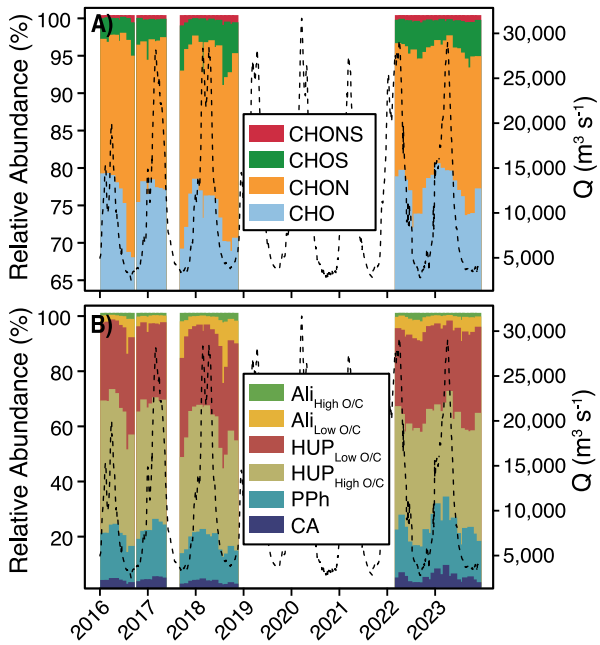

Figure 5. Compound classes derived from FT-ICR MS molecular formulae in Tapajós River water samples during 2016–2018 and 2022–2023 are depicted as percentage relative abundance. Molecular formulae are colored according to: (a) heteroatom class (CHO, blue; CHON, orange; CHOS, green; CHONS, red) and (b) compound classes condensed aromatic (CA), dark blue; polyphenolic (PPh), light blue; highly unsaturated and phenolic low O/C ($HUP_{Low\ O/C}$), tan; HUP high O/C ($HUP_{High\ O/C}$), red; aliphatic low O/C ($Ali_{Low\ O/C}$), orange; aliphatic high O/C ($Ali_{High\ O/C}$), green. Discharge (Q) is indicated by the dashed black line.

compound class trends with discharge and are similar to compositions at peak discharge near the mixing zone (Figures S6a–S6e in Supporting Information S1; S. Li, Harir, Schmitt-Kopplin, Machado-Silva, et al., 2023). IOS relative abundance (14.1–22.6, mean: 17.3%) was highest in July and lowest in April (Figure S6f in Supporting Information S1) and followed Amazon River seasonality (Kurek et al., 2022).

3.6. PARAFAC Modeling

All five PARAFAC components were validated using split halves (Figure S7 in Supporting Information S1) and matched to previously identified fluorophores in the OpenFluor database that are summarized in Table S2 in Supporting Information S1. C1 ($Ex_{240,320}$, Em_{440}) and C2 ($Ex_{245,410}$, Em_{525}) were similar to humic-like terrestrial fluorophores and C3 ($Ex_{268,375}$, Em_{462}) is thought to represent soil organic matter (Table S2 in Supporting Information S1). C1–C3 all correlated positively with CDOM and DOM properties from absorbance and FT-ICR MS spectra linked to aromaticity (Table S3 in Supporting Information S1). C4 ($Ex_{<240,290}$, Em_{382}) is similar to microbial humic-like peak M and potentially related to aquatic production while C5 ($Ex_{<240,273}$, Em_{309}) is similar to tyrosine-like fluorophores (Table S2 in Supporting Information S1). Both C4 and C5 correlated negatively with aromatic DOM properties and positively with heteroatom content (Table S3 in Supporting Information S1).

The sum of all fluorescent component intensity maxima (FDOM) varied with discharge and peaked between December and February on the rising limb and was the lowest between August-September (Figure 6a). The proportions of C1 (20-2-55.7, mean: 46.0%), C2 (6.5–20.8, mean: 15.9%), and C3 (3.6–13.4, mean: 10.5%) were all highest from January-April and lowest from July-September while C4 (8.4–14.5, mean: 25.8%) and C5 (0–59.6, mean: 13.1%) followed the inverse (Figure 6b).

3.7. LOADEST Fluxes

The mean annual discharge flux from the Tapajós River was 349 ± 48 km^3 yr^{-1} (Table 1). The mean annual DOC flux was 1.38 ± 0.24 Tg C yr^{-1} and the mean DOC yield was 2.82 ± 0.50 g C yr^{-1} m^{-2} (Table 1). DOC fluxes were strongly driven by both DOC concentrations and instantaneous discharge with the highest fluxes during peak discharge and the lowest at minimum discharge (Figure 7a). Average annual DOC fluxes were greater than previous estimates from samples taken downstream of Itaituba (1.29 ± 1.39 Tg C yr^{-1}; Moreira-Turcq et al., 2003). The mean annual CDOM flux was 3.30 ± 0.46 g C yr^{-1} m^{-2} and the CDOM yield was 6.69 ± 0.93 $years^{-1}$ (Table 1). Similarly to DOC, monthly CDOM fluxes were seasonal and generally followed discharge (Figure 7b). LOADEST model fluxes (black lines) were comparable to instantaneous fluxes calculated from discharge and analyte concentration at each sampling day (Figures 7a and 7b; red points) with a strong correlation ($r^2 = 0.91$).

4. Discussion

Overall, the Tapajos River basin experiences similar annual temperature and precipitation averages to other clearwater tributaries such as the Xingu, Trombetas, and Tocantins as well as the Amazon River basin upstream of Óbidos (Drake et al., 2021; Moreira-Turcq et al., 2003; Neu et al., 2023; Panday et al., 2015; Figure S3 in Supporting Information S1). However, seasonal patterns across the Tapajós River basin are more pronounced than those across the Amazon River, particularly during the low discharge periods. For instance, the Tapajós River had a much larger mean intra-annual variability (8.77, max Q/min Q) compared to the Amazon River (2.93) and on average, precipitation was 4.2 times greater than specific discharge (Figure 3a), whereas it was only about double across the Amazon basin (Drake et al., 2021). Furthermore, peak monthly precipitation often coincided with peak discharge in the Tapajós River, in contrast to the Amazon River, which often experiences a 3 to 4-month

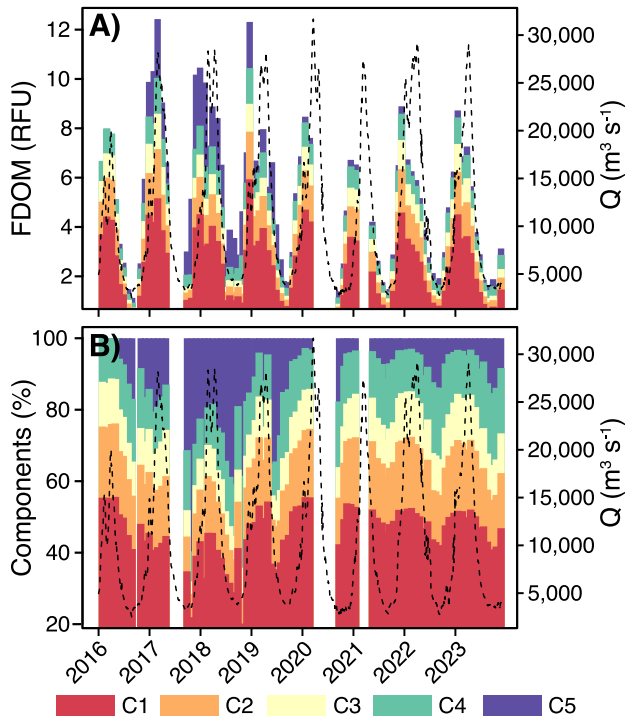

Figure 6. PARAFAC components (C1-C5) modeled from the Tapajós River water samples during 2016–2023. (a) Components are represented in relative fluorescence units and (b) as percent composition of total fluorescence maxima. Components are colored according to the following: C1, red; C2, orange; C3, yellow; C4, green; C5, blue. Discharge (Q) is indicated by the dashed black line.

lag (Marengo, 2006; Richey et al., 1989). This suggests differences in rainwater delivery and discharge loss between the two river basins where more precipitation (~75%) is lost across the Tapajós River basin as evapotranspiration. Such differences are largely due to the large basin area and geographical positioning of the Amazon River, which integrates river systems from both southern and northern tributaries. As the headwaters of northern tributaries originate north of the equator, they experience wet seasons and peak discharge in different months than the southern tributaries, such as the Tapajós River (Richey et al., 1989; Sioli, 1984). Regardless, carbon export in both river systems is driven by the flood pulse and we discuss the role of seasonality in the Tapajós River based on the phases of the hydrograph.

4.1. Seasonality of Tapajós River Discharge, DOC, and DOM Export

Rising discharge typically occurs from November-February when precipitation increases to its peak and air temperatures decrease to their minima (Figures 2b and S3 in Supporting Information S1). This period is characterized by a nearly equal increase in the rate of precipitation and discharge from the event water (Figure 3a), which becomes more depleted as relatively depleted rainwater is incorporated into the river (Mortatti et al., 1997). Riverine DOC concentrations, CDOM and FDOM are highest during this period (Figures 4 and 6a), indicating that sustained precipitation increases landscape connectivity and mobilizes organic carbon from litter layers into the river (Dalmagro et al., 2017; Lambert et al., 2016; Seidel et al., 2016). This is also supported by the positive clockwise direction of DOC-Q and CDOM-Q relationships (Figure S5 in Supporting Information S1), indicating that terrestrial sources are spatially connected to each other and the river (Creed et al., 2015). Additionally, most of this DOM is compositionally aromatic and terrestrial with high $SUVA_{254}$, greater proportions of C1-C3 fluorophores, and $HUP_{High\ O/C}$ compounds (Figures 4b, 5b, and 6b), suggesting this DOM is flushed from surface soils and connected surface waters (de Melo et al., 2020; Hertkorn et al., 2016; Kurek et al., 2022; Seifert et al., 2016). Terrestrial delivery into the Tapajós River continues through peak discharge (March–April) as the proportion of this DOM pool remains high and flow paths are further expanded thereby increasing CA and PPh delivery (Figure 5b). These DOM formulae are highly aromatic and often associated with forest cover and leached vegetation (Spencer et al., 2019; Textor et al., 2018; Wagner et al., 2019), suggesting that inundated vegetation and wetland forests (igapó) could be significant sources of terrestrial DOM to the Tapajós River at maximum discharge. However, we note that the Tapajós River lacks large floodplains compared to the Amazon River and thus this sourcing is likely confined to the headwaters during a

Table 1
Annual Discharge (Q), Dissolved Organic Carbon (DOC), and CDOM (a_{350}) Fluxes as Well as DOC and CDOM Yields From the Tapajós River During 2016–2023

	Q ($km^3\ yr^{-1}$)	DOC flux (Tg C yr^{-1})	a_{350} flux ($10^{12}\ m^2\ yr^{-1}$)	DOC yield (g C $yr^{-1}\ m^{-2}$)	a_{350} yield (yr^{-1})
2016	245	1.10	2.4	2.24	4.88
2017	352	1.66	3.6	3.40	7.33
2018	380	1.71	3.7	3.48	7.63
2019	375	1.54	3.5	3.14	7.20
2020	352	1.31	3.2	2.68	6.56
2021	334	1.21	3.1	2.48	6.25
2022	406	1.44	3.7	2.93	7.55
2023	350	1.08	3.0	2.21	6.13
Mean ± SD	349 ± 48	1.38 ± 0.24	3.3 ± 0.46	2.82 ± 0.50	6.69 ± 0.93
Percent of Amazon River (%)	6.1	5.4	4.4		

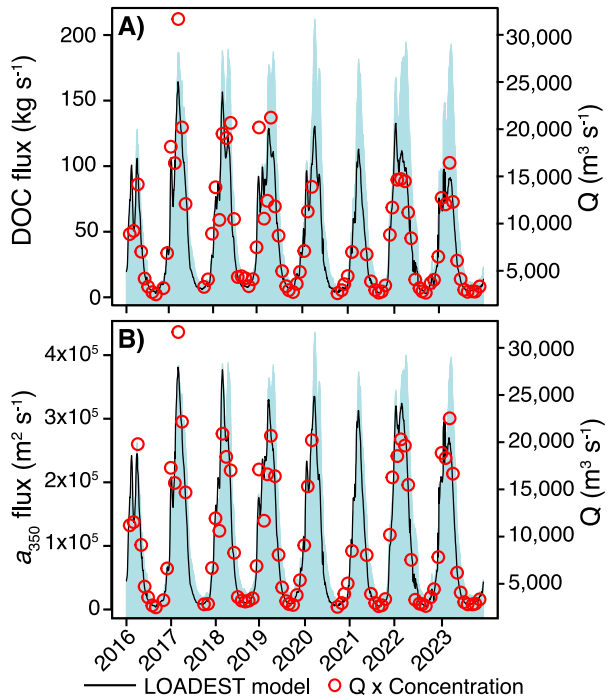

Figure 7. Time series of instantaneous discharge (Q, blue shaded region), LOADEST model fluxes (black lines), and measured fluxes (red open points) for (a) dissolved organic carbon concentration and (b) CDOM absorption at 350 nm (a_{350}) during 2016–2023.

relatively brief period of time as well as from marginal lakes formed alongside the river (de Paiva et al., 2013). This may further explain differences in terrestrial DOM composition between the Tapajós and Amazon River (e.g., Ward et al., 2015) as well as differences in forest cover since igapó vegetation typically has lower productivity and biomass than the várzea of the Amazon mainstem (Junk et al., 2011).

From May-July, discharge steadily decreased with precipitation while air temperatures began to rise (Figures 2b and S3 in Supporting Information S1). During the falling limb, nearly all additional rainwater was exported as discharge but not replenished (1:1 line, Figure 3a). At the beginning of the falling limb, this additional rainwater was relatively enriched in heavy isotopes (Figures 3c and 3d), causing minor enrichment in the river water upon mixing and export (Martinelli et al., 1996; Mortatti et al., 1997). However, between June and July, less evaporated water was retuned as precipitation and the river began drying, enriching the remaining river water in heavy isotopes (Figures 3c and 3d). This is further supported by the variations in D-excess in the Tapajós River, which ranged between 9.8 and 10.6 from January to May but decreased to 7.9 by July (Figure S3c in Supporting Information S1). As the discharge decreased, flow paths became disconnected from the landscape and less organic carbon was mobilized into the Tapajós, resulting in lower overall DOC, CDOM, and FDOM (Figures 4a, 6a, and S5 in Supporting Information S1). This DOM was compositionally more aliphatic with higher $S_{275–295}$, $\%Ali_{Low\ O/C}$, H/C (Figures 3b and 5b, and S6a in Supporting Information S1) and less oxygenated (lower average O/C and NOSC; Figures S6b and S6d in Supporting Information S1). These signatures are consistent with aquatic microbial and autochthonous DOM (Kurek et al., 2020; Osterholz et al., 2016; Riedel et al., 2016) and could be related to increased microbial processing of recently mobilized fresh terrestrial DOM following peak landscape connectivity (de Melo et al., 2020; Lapierre & Del Giorgio, 2014). IOS relative abundance also peaked at this time (Figure S6f in Supporting Information S1) and given its significant correlation with C4 (Table S3 in Supporting Information S1), suggests that a greater proportion of DOM exported during this time has undergone microbial processing compared to high discharge periods (Kurek et al., 2022; Lechtenfeld et al., 2014). Additionally, these formulae could also represent stable aged DOM sourced from deeper flow paths or groundwater (Kellerman et al., 2018; McDonough et al., 2022) as the Tapajós River typically has greater average groundwater contributions to discharge than the Amazon mainstem (de Paiva et al., 2013).

Microbial DOM persisted through the minimum discharge period (August-October) when average temperatures were at their highest and before monthly precipitation began increasing again (Figures 2b and S3 in Supporting Information S1). The Tapajós River experienced widespread evaporative drying during this time as river water isotopes became rapidly enriched and D-excess reached minimum values (6.3–6.7‰) with no appreciable increase in discharge, indicating removal of event water (Figures 3c and 3d; Martinelli et al., 1996; Tardy et al., 2005). Warm air temperatures, optical clarity, and stagnating waters likely promoted algal growth in the Tapajós River, as has been previously observed (Doherty et al., 2017; Ward et al., 2015, 2016), and exported DOM characterized by high FI and C5 proportions with greater relative abundance of N,S-containing formulae (Figures 4d–6b). These DOM compositional changes reflect the transition between passive DOM delivery during high discharge periods and active processing during reduced flow within the Tapajós River network as driven by the seasonal food pulse (Raymond et al., 2016).

The flood pulse is also significantly influenced by extreme dry periods and a longer accumulation time of precipitation within the landscape prior to discharge, in contrast to the Amazon River, which rapidly incorporates event water during the rising limb and efficiently recycles rainwater between the river and atmosphere (Drake et al., 2021; Mortatti et al., 1997). These cycles of precipitation and drying alter the molecular composition of exported DOM from the Tapajós River. For instance, molecular formulae positively correlated with $\delta^{18}O$ were highly aliphatic and enriched in N,S-containing formulae while negatively correlated formulae consisted of CA and PPh compounds (Figures 8a and 8b). This illustrates the molecular fingerprint of aromatic DOM mobilized

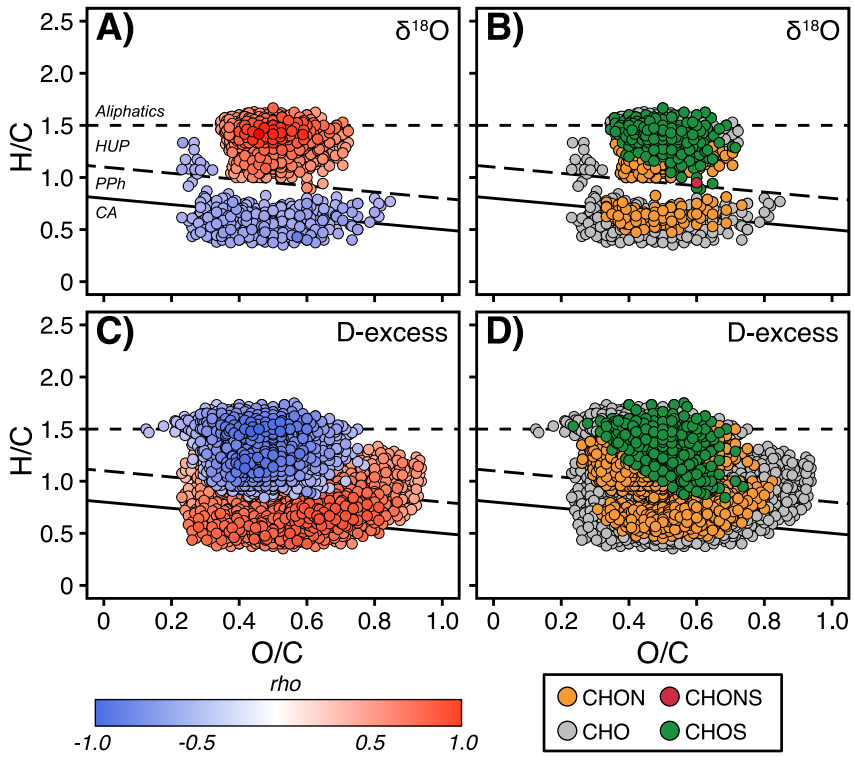

Figure 8. van Krevelen diagrams depicting the spearman correlations between individual FT-ICR MS formulae and: (a, b) $\delta^{18}O$ and (c, d) D-excess. Positively correlated formulae in panels (a, c) are colored in red and negatively correlated formulae are in blue. Molecular formulae are also colored according to heteroatom class in panels (b, d) (CHO, gray; CHON, orange; CHOS, green; CHONS, red). Compound class regions are denoted by dashed/solid lines and include: aliphatics, highly unsaturated and phenolic (HUP), polyphenolic (PPh), and condensed aromatic (CA).

from connected soils and inundated vegetation following peak precipitation and those prevalent in the river during low precipitation and high evaporative periods, that is, the two most abundant endmembers of Tapajós River DOM. Similarly, molecular formulae positively correlated with D-excess spanned O/C ranges typical of major world rivers, such as the Amazon and Congo (Kurek et al., 2022; Riedel et al., 2016; Wagner et al., 2015), but were shifted to lower H/C ranges, suggesting DOM incorporation from many terrestrial sources during periods of evaporative recycling across the basin (Martinelli et al., 1996; Tardy et al., 2005). Negatively correlated formulae had higher H/C and lower O/C ratios, and were enriched in N,S-containing formulae (Figures 8c and 8d), similar to what has been observed in algal leachates and bloom-impacted lakes (Patriarca et al., 2021; Zhang et al., 2014). These correlations indicate that during high evaporative periods (low D-excess) the terrestrial supply to the Tapajós River is attenuated, and the river behaves like a lake with long water residence times that exports algal DOM with a greater potential for in-stream processing.

4.2. Carbon Delivery to the Amazon River

We estimate that the Tapajós River exports approximately 1.38 Tg C annually from Itaituba with the potential to increase total Amazon River DOC and CDOM exports by up to 5.4% and 4.4%, respectively (Table 1; Drake et al., 2021). Combining the DOC fluxes of the Tapajós (1.38), Tocantins (0.85; Neu et al., 2023), and estimates from the Xingu (0.59 Tg C yr^{-1}; Panday et al., 2015; Ward et al., 2016), the southeastern Amazon basin delivers an additional 2.82 Tg DOC to the Amazon River network downstream of Óbidos, amounting to more DOC than is exported by the Mississippi each year (2.10 Tg C yr^{-1}; Spencer & Raymond, 2024). This additional amount is important to consider for global riverine fluxes as well as residence time calculations of terrestrial DOC in the Atlantic Ocean to better constrain land-ocean carbon cycling.

The Tapajós River exports less DOC annually (1.38 Tg C) than the largest tributaries of the Amazon River such as the Rio Negro (5.2–8.1) and Madeira River (2.9–4.3; Guinoiseau et al., 2016; Richey et al., 1990; Seyler

et al., 2005); however, this amount is still similar to some of the largest rivers on Earth including the Mekong (1.11), Yukon (1.47), Mackenzie (1.38), and Yangtze River (1.58 Tg C y^{r-1}; Spencer & Raymond, 2024). Additionally, the DOC yield of the Tapajós River (2.8 g C yr^{-1} m^{-2}; Table 1) is more than double the areal yield of the Tocantins River (1.1 g C yr^{-1} m^{-2}; Neu et al., 2023) and higher than the estimated global average for the 30 largest rivers by discharge (2.3 g C yr^{-1} m^{-2}; Spencer & Raymond, 2024). Rivers with higher DOC yields are primarily large tropical systems such as the Amazon and the Orinoco (5.5, 4.5 g C yr^{-1} m^{-2}, respectively; Coynel et al., 2005; Drake et al., 2021; Spencer & Raymond, 2024), as well as smaller tropical blackwater rivers dominated by forests and wetlands including the Rio Negro (8.7 g C yr^{-1} m^{-2}; Coynel et al., 2005) and Ogooue River (6.1; g C yr^{-1} m^{-2}; Spencer & Raymond, 2024). This suggests that despite its clearwater characteristics (low DOC and CDOM), the Tapajós River is an efficient organic carbon exporter for its watershed size and is likely influenced by its high percent forest coverage (50%) compared to other clearwater rivers such as the Tocantins (Neu et al., 2023).

Although we demonstrated that DOM is incorporated from various sources across the seasonal hydrograph, the overall composition of Tapajós River DOM determined via optical (Figures 4b–4d), fluorescence (Figure 6), and FT-ICR MS (Figures 5 and S6 in Supporting Information S1) indices is more algal and/or microbial in nature compared to the Amazon River mainstem and other tributaries (Gonsior et al., 2016; Kurek et al., 2022; S. Li, Harir, Schmitt-Kopplin, Gonsior, et al., 2023; Seidel et al., 2016; Simon et al., 2021). DOM with algal and/or microbial signatures is preferentially utilized for microbial respiration on short timescales (Guillemette et al., 2013; Patriarca et al., 2021) and suggests that the Tapajós River exports overall more biolabile DOM, particularly during falling and low discharge (Figures 6b and 8). This supports previous findings that suggested clearwater rivers (e.g., Tapajós and Xingu) are likely important contributors of exported algal and microbial organic matter to the lower Amazon River network (Rosengard et al., 2024; Seidel et al., 2016; Ward et al., 2015). Delivery of this autochthonous DOM to the Amazon River confluence impacts downstream CO_2 evasion as it could enhance respiration of terrestrial DOM in the Amazon mainstem via priming (Ward et al., 2016).

However, the proportion of this DOM passing through Itaituba that is truly exported into the Amazon River is unknown as this water mass experiences different biological and physiochemical conditions across the slow-moving Tapajós Ria and within the Amazon mixing zone (Doherty et al., 2017; Ward et al., 2016). Thus of the 1.38 Tg C exported annually from the Tapajós at Itaituba, it is unknown how much is delivered to the Amazon River downstream from the Tapajós Ria, as we recognize the potential for significant in-stream processing as well as input of additional carbon sources. The Tapajós Ria itself is a dynamic part of the Amazon River carbon cycle (e.g., Sawakuchi et al., 2017) and we expect DOM exported across the Amazon mixing zone to experience compositional changes, particularly during low discharge periods as biolabile component C5 (Figure 6) and oxygenated species ($Ali_{High\ O/C}$, $HUP_{High\ O/C}$, Figure 5b) that were delivered from Itaituba are consumed. The Ria may also incorporate additional DOM sources from the Arapiuns River near the Amazon mixing zone in this region, and internally via primary production, which may increase DOC fluxes. For instance, delivery of nutrients from the Tapajós watershed into the Ria may stimulate algal/cyanobacterial production within the Tapajós Ria (de Moraes Novo et al., 2006; Torres et al., 2020), exporting additional DOC into the mixing zone. As the rivers mix, DOM undergoes rapid processing whereby high O/C formulae are preferentially consumed and distinct aliphatic formulae are produced (S. Li, Harir, Schmitt-Kopplin, Machado-Silva, et al., 2023), which may be further incorporated into the lower reaches of the Amazon and respired.

4.3. Interannual Variations

In addition to seasonal trends in organic carbon sourcing, interannual DOC export and DOM composition varied across the study period. Annual DOC, and CDOM fluxes were lower in 2016 compared to the average due to lower DOC concentrations and CDOM (Figure 3a), and reduced discharge fluxes in 2016 (Table 1; Figure 7). While peak precipitation in 2016 was similar to the following years, less precipitation had accumulated during the dry season between July-December 2015 compared to long term averages (Figure 2a; Van Schaik et al., 2018). As most of the terrestrial water in the Tapajós River basin is stored in soils rather than surface water (de Paiva et al., 2013), the landscape absorbed more precipitation during the wet season (January-March) resulting in less runoff and flushing of terrestrial organic matter. These precipitation changes were likely influenced by the massive 2015 El Niño event that caused droughts and widespread wildfires across the eastern Amazon, including large portions of the lower Tapajós River watershed (Berenguer et al., 2021; Jiménez-Muñoz et al., 2016). Previous studies have also identified the effects of ENSO-driven climate anomalies on riverine DOC export and

suggested that changes in flow paths alter DOM sourcing across the watershed (e.g., Kurek et al., 2021; Qu et al., 2020). Since sampling began in 2016 after the most severe impacts of the drought on the Tapajós River basin, average DOM composition was largely unaffected after peak discharge as flow paths were maintained and DOC fluxes increased the following years (Table 1).

From 2017 to 2018, DOM exported from the Tapajós River was noticeably less aromatic with lower proportions of C1-C3 (Figure 6b), HUP compounds (Figure 5b), and lower $SUVA_{254}$ (Figure 3c). Instead, DOM was more aliphatic with steeper $S_{275–295}$, higher FI (Figures 3c and 3d), greater proportions of C5 (Figure 6b), Ali, and N- and S-containing formulae (Figures 5a and 5b). Furthermore, linear regressions between DOC and CDOM suggested that the sourcing of DOM changed during this period as well (Figure S8 in Supporting Information S1). For most years, the slope of the DOC-CDOM regression was 2.79, which is similar to that of the Amazon mainstem (2.68; Drake et al., 2021). However, from 2017 to 2018, the slope of the relationship decreased to 2.00 and 1.97, respectively (Figure S8 in Supporting Information S1), and was similar to temperate rivers such as the Colorado River (1.83) or Hudson River (2.05), which incorporate less terrestrial DOM from their watersheds (Spencer et al., 2012). This change in sourcing could possibly be related to heightened algal/cyanobacterial production as well as degradation of terrestrial DOM during transport, thereby reducing bulk aromaticity relative to DOC concentrations. In 2017, positive rainfall anomalies and convergent water vapor fluxes were concentrated in the northern and northeastern Amazon basins, while the southeastern and Cerrado regions experienced a drought (Espinoza et al., 2022). Such conditions, along with sediment inputs from mine tailings (Lobo et al., 2016) could have stimulated algal productivity in the southern and eastern tributaries and exported an excess of algal DOM compared to what was typical across the study period (Figure S8 in Supporting Information S1). Eutrophic conditions and blooms have been observed in the Tapajós River previously (Costa et al., 2013; Lobo et al., 2017; Sioli, 1984) with phytoplankton activity in the river likely contributing to production in the connected Amazon floodplain during low water periods (de Moraes Novo et al., 2006; Rosengard et al., 2024). Therefore, it is possible that periodic bloom periods in the Tapajós River network could be important mechanisms for delivering biolabile DOM to the Tapajós Ria and Amazon mixing zone, enhancing aquatic respiration. Drought conditions could also have enhanced microbial processing of DOM from the surrounding watershed, sourced from soils and connected wetlands, altering the composition of terrestrial DOM flushed into the river during runoff events and resulting in a shallower DOC-CDOM slope (Figure S8 in Supporting Information S1). These findings highlight the need for multi-year studies in tropical rivers as even these systems that are thought to be stable experience great variability in DOM export.

4.4. Anthropogenic Impacts

Land conversion across Pará and Mato Grosso states has significantly altered the hydrology of the Tapajós River basin (Castello & Macedo, 2016; Farinosi et al., 2019; Lobo et al., 2016; Pavanato et al., 2016) as well as the carbon cycle of the Amazon system (Davidson et al., 2012; Fearnside, 2018). Ongoing deforestation has impacted ecosystems and soil composition across the basin with ramifications for soil organic matter content and riverine export (Bernardes et al., 2004; Souza et al., 2024; Spencer et al., 2019). Prior to intensified deforestation, suspended sediment organic matter in the Tapajós River was mostly sourced from forested vegetation, whereas it has since transitioned to soil organic matter and subsurface particulates (Farella et al., 2001). Similarly, deforestation and mining have altered the water quality of the Tapajós River through increased runoff, resulting in higher suspended solids (Lobo et al., 2016), DOC, and dissolved solutes (Nóbrega, Guzha, et al., 2018; Nóbrega, Lamparter, et al., 2018).

Throughout this study period we have also observed changes in the landscape across the Tapajós River basin as the coverage of grasslands and croplands has increased at the expense of savanna and forest cover (Figure S9 in Supporting Information S1). This was accompanied by a significant change in the optical and fluorescent DOM composition via spearman correlations. We note a significant negative correlation between CDOM and the ratio of grassland to savanna and grasslands to forest (rho = −0.82) and a significant positive correlation with %C4 (rho = 0.82) with similar trends for cropland (Table S4 in Supporting Information S1). This suggests that expansion of grassland and cropland at the expense of savanna tree cover mobilizes less aromatic DOM from litter layers and more microbially processed DOM into connected river networks. Whether the microbially processed C4 fluorophores originated from degradation of exposed soil or were byproducts of soil DOM that was processed during transport is unknown. However, given that C3, which was previously linked to soil organic matter, did not correlate significantly with landcover, and it is likely that C4 is linked to DOM processed within the river

network. Furthermore, Amazonian soils from primary forests typically contain more aliphatic and biolabile organic matter than deforested soils, suggesting that these components were consumed in the headwaters of the river network (Souza et al., 2024). We also recognize that these correlations represent monotonic trends that cannot be used quantitatively and that watershed land use proportions are heterogenous, meaning that stronger relationships may exist within specific sub-basins or tributaries undergoing more intensive land conversion. Additionally, there may be other unidentified parameters across the study period that are responsible for these trends, including inputs from point sources, with additional studies needed to assess their impacts on DOC export from this region.

However, these temporal changes to DOM composition reflect the susceptibility of the Amazon system to external drivers. Similar findings were observed with the expansion of soybean crops across the headwaters of the Xingu River, where forest cover was strongly correlated with highly aromatic molecular formulae, while cropland coverage was positively correlated with low O/C and N-containing molecular formulae, similar to the IOS (Spencer et al., 2019). Others have reported ^{14}C-depleted dissolved black carbon (DBC) exported from the Tapajós River, indicating significant incorporation of fossil fuel combustion byproducts, despite the prevalence of modern DBC upstream of the Amazon River (Coppola et al., 2019). These observations along with our findings suggest that there is a strong anthropogenic component to the DOM signature in the Tapajós River and possibly other clearwater rivers downstream of the Amazon, which could be traced using molecular indices.

The Tapajós River basin is expected to become hotter and drier in the coming decades, causing riverine discharge to decrease and a delay in the onset of the wet season (Farinosi et al., 2019). Additionally, the effects of land use change increase runoff potential (da Silva Cruz et al., 2022) and introduce considerable intra- and interannual variability to discharge and export (Aufdenkampe et al., 2011; Farinosi et al., 2019; Lobo et al., 2016). This means that future DOC fluxes to the Amazon River and DOM composition will be influenced by both the changing hydrologic cycle and anthropogenic impacts. Given the combined effects of drying and land conversion, it is likely that the Tapajós River may export more biolabile algal and microbial DOM from its watershed, potentially increasing respiration in the Amazon mixing zone and downstream river network. Therefore, additional work is needed to understand the regional effects of climate anomalies and specific land use on clearwater Amazonian rivers and their contributions to the entire Amazon basin.

5. Conclusion

This study presented a comprehensive analysis of continuous hydrological parameters, carbon fluxes, and DOM composition of the Tapajós River for 8 years between 2016 and 2024. We identified strong seasonal patterns in the flood pulse and evaporation within the river related to changes in precipitation and temperature throughout the basin. Similar to the Amazon River, this seasonal flood pulse was the primary driver for exporting DOC and terrestrial DOM during periods of high hydrologic connectivity. In contrast, high temperatures and drought conditions reduced overall DOC export in the low discharge months but increased the proportion of DOM originating from microbial processing and algal production. We report that the Tapajós River exports 1.38 Tg C DOC annually at Itaituba to the Tapajós Ria and Amazon mixing zone, representing a similar amount of DOC that is exported annually from the Yukon or Mekong River. Given that Tapajós River DOM is aliphatic and likely biolabile in short timescales, this exported DOM potentially fuels processing and respiration across the Amazon mixing zone, delivering unique signatures into the downstream Amazon River network. We also report inter-annual variations in DOC export and DOM composition as related to large scale climate anomalies such as the 2015 El Niño as well as localized droughts in the headwaters. Decreased runoff from the El Niño event reduced discharge and DOC fluxes the following year, while hot and dry conditions most likely promoted regional blooms in the southern tributaries that increased the algal signature of DOM exported at Itaituba. Finally, an increase in basin-wide grassland and croplands at the expense of savanna over this study period correlated significantly with decreases in CDOM and increases in the microbially processed DOM component C4. This suggests that anthropogenic land use changes in the Tapajós River basin have the potential to impact aquatic DOM processing and export to the Amazon River. Future changes in the Amazonian hydrologic cycle and continued anthropogenic impacts such as deforestation and mining will thus be traceable in clearwater tributaries and impact carbon cycling in the lower reaches of the Amazon River.

Conflict of Interest

The authors declare no conflicts of interest relevant to this study.

Data Availability Statement

The authors declare that all data measurements supporting the results of this study have been uploaded as supporting Data Set S1 in the supplemental information and uploaded to the Open Science Framework (OSF). All landcover classifications, FT-ICR MS spectra, and assigned molecular formulae associated with this study are also archived in the OSF (Kurek, 2025; https://doi.org/10.17605/OSF.IO/USH6Y).

Acknowledgments
R.G.M.S. and M.R.K. acknowledge support from the NSF RAPID Award 2333961. A portion of this work was performed at the National High Magnetic Field Laboratory ICR User Facility, which is supported by the National Science Foundation Division of Chemistry and Division of Materials Research through DMR-2128556 and the state of Florida. We thank Anya Suslova for laboratory and sample assistance and Travis Drake for advice on LOADEST modeling. We acknowledge the analytical support by the IAEA Isotope Hydrology Laboratory and its staff through the Global Network of Isotopes in Rivers (GNIR). We also acknowledge the early work and efforts of Renata Silva Souza on the Tapajós River prior to sampling for this project.

References

Albéric, P., Pérez, M. A. P., Moreira-Turcq, P., Benedetti, M. F., Bouillon, S., & Abril, G. (2018). Variation of the isotopic composition of dissolved organic carbon during the runoff cycle in the Amazon River and the floodplains. *Comptes Rendus Geoscience*, *350*(1–2), 65–75. https://doi.org/10.1016/j.crte.2017.11.001

Amon, R. M. W., & Benner, R. (1996). Bacterial utilization of different size classes of dissolved organic matter. *Limnology & Oceanography*, *41*(1), 41–51. https://doi.org/10.4319/lo.1996.41.1.0041

Aufdenkampe, A. K., Mayorga, E., Hedges, J. I., Llerena, C., Quay, P. D., Gudeman, J., et al. (2007). Organic matter in the Peruvian headwaters of the Amazon: Compositional evolution from the Andes to the lowland Amazon mainstem. *Organic Geochemistry*, *38*(3), 337–364. https://doi.org/10.1016/j.orggeochem.2006.06.003

Aufdenkampe, A. K., Mayorga, E., Raymond, P. A., Melack, J. M., Doney, S. C., Alin, S. R., et al. (2011). Riverine coupling of biogeochemical cycles between land, oceans, and atmosphere. *Frontiers in Ecology and the Environment*, *9*(1), 53–60. https://doi.org/10.1890/100014

Battin, T. J., Lauerwald, R., Bernhardt, E. S., Bertuzzo, E., Gener, L. G., Hall, R. O., et al. (2023). River ecosystem metabolism and carbon biogeochemistry in a changing world. *Nature*, *613*(7944), 449–459. https://doi.org/10.1038/s41586-022-05500-8

Battin, T. J., Luyssaert, S., Kaplan, L. A., Aufdenkampe, A. K., Richter, A., & Tranvik, L. J. (2009). The boundless carbon cycle. *Nature Geoscience*, *2*(9), 598–600. https://doi.org/10.1038/ngeo618

Benjamini, Y., & Hochberg, Y. (1995). Controlling the false discovery rate: A practical and powerful approach to multiple testing. *Journal of the Royal Statistical Society: Series B*, *57*(1), 289–300. https://doi.org/10.1111/j.2517-6161.1995.tb02031.x

Berenguer, E., Lennox, G. D., Ferreira, J., Malhi, Y., Aragão, L. E. O. C., Barreto, J. R., et al. (2021). Tracking the impacts of El Niño drought and fire in human-modified Amazonian forests. *Proceedings of the National Academy of Sciences*, *118*(30), e2019377118. https://doi.org/10.1073/pnas.2019377118

Berggren, M., Guillemette, F., Bieroza, M., Buffam, I., Deininger, A., Hawkes, J. A., et al. (2022). Unified understanding of intrinsic and extrinsic controls of dissolved organic carbon reactivity in aquatic ecosystems. *Ecology*, *103*(9), e3763. https://doi.org/10.1002/ecy.3763

Bernardes, M. C., Martinelli, L. A., Krusche, A. V., Gudeman, J., Moreira, M., Victoria, R. L., et al. (2004). Riverine organic matter composition as a function of land use changes, southwest Amazon. *Ecological Applications*, *14*(sp4), 263–279. https://doi.org/10.1890/01-6028

Bertassoli, D. J., Sawakuchi, A. O., Sawakuchi, H. O., Pupim, F. N., Hartmann, G. A., McGlue, M. M., et al. (2017). The fate of carbon in sediments of the Xingu and Tapajós Clearwater Rivers, eastern Amazon. *Frontiers in Marine Science*, *4*. https://doi.org/10.3389/fmars.2017.00044

Boye, K., Noël, V., Tfaily, M. M., Bone, S. E., Williams, K. H., Bargar, J. R., & Fendorf, S. (2017). Thermodynamically controlled preservation of organic carbon in floodplains. *Nature Geoscience*, *10*(6), 415–419. https://doi.org/10.1038/ngeo2940

Bustillo, V., Victoria, R. L., de Moura, J. M. S., de Victoria, D. C., Toledo, A. M. A., & Colicchio, E. (2011). Biogeochemistry of carbon in the Amazonian floodplains over a 2000-km reach: Insights from a process-Based model. *Earth Interactions*, *15*(4), 1–29. https://doi.org/10.1175/2010EI338.1

Castello, L., & Macedo, M. N. (2016). Large-scale degradation of Amazonian freshwater ecosystems. *Global Change Biology*, *22*(3), 990–1007. https://doi.org/10.1111/gcb.13173

Cole, J. J., Prairie, Y. T., Caraco, N. F., McDowell, W. H., Tranvik, L. J., Striegl, R. G., et al. (2007). Plumbing the global carbon cycle: Integrating inland waters into the terrestrial carbon budget. *Ecosystems*, *10*(1), 172–185. https://doi.org/10.1007/s10021-006-9013-8

Coplen, T. B., & Wassenaar, L. I. (2015). LIMS for Lasers 2015 for achieving long-term accuracy and precision of δ2 H, δ17 O, and δ18 O of waters using laser absorption spectrometry: LIMS for Lasers 2015. *Rapid Communications in Mass Spectrometry*, *29*(22), 2122–2130. https://doi.org/10.1002/rcm.7372

Coppola, A. I., Seidel, M., Ward, N. D., Viviroli, D., Nascimento, G. S., Haghipour, N., et al. (2019). Marked isotopic variability within and between the Amazon River and marine dissolved black carbon pools. *Nature Communications*, *10*(1), 4018. https://doi.org/10.1038/s41467-019-11543-9

Corilo, Y. (2014). PetroOrg [Computer Software]. https://perto.org

Cory, R. M., & McKnight, D. M. (2005). Fluorescence spectroscopy reveals ubiquitous presence of oxidized and reduced quinones in dissolved organic matter. *Environmental Science & Technology*, *39*(21), 8142–8149. https://doi.org/10.1021/es0506962

Cory, R. M., Miller, M. P., McKnight, D. M., Guerard, J. J., & Miller, P. L. (2010). Effect of instrument-specific response on the analysis of fulvic acid fluorescence spectra. *Limnology and Oceanography: Methods*, *8*(2), 67–78. https://doi.org/10.4319/lom.2010.8.67

Costa, M. P. F., Novo, E. M. L. M., & Telmer, K. H. (2013). Spatial and temporal variability of light attenuation in large rivers of the Amazon. *Hydrobiologia*, *702*(1), 171–190. https://doi.org/10.1007/s10750-012-1319-2

Coynel, A., Seyler, P., Etcheber, H., Meybeck, M., & Orange, D. (2005). Spatial and seasonal dynamics of total suspended sediment and organic carbon species in the Congo River. *Global Biogeochemical Cycles*, *19*(4), 2004GB002335. https://doi.org/10.1029/2004GB002335

Creed, I. F., McKnight, D. M., Pellerin, B. A., Green, M. B., Bergamaschi, B. A., Aiken, G. R., et al. (2015). The river as a chemostat: Fresh perspectives on dissolved organic matter flowing down the river continuum. *Canadian Journal of Fisheries and Aquatic Sciences*, *72*(8), 1272–1285. https://doi.org/10.1139/cjfas-2014-0400

Dalmagro, H. J., Johnson, M. S., de Musis, C. R., Lathuillière, M. J., Graesser, J., Pinto-Júnior, O. B., & Couto, E. G. (2017). Spatial patterns of DOC concentration and DOM optical properties in a Brazilian tropical river-wetland system. *Journal of Geophysical Research: Biogeosciences*, *122*(8), 1883–1902. https://doi.org/10.1002/2017JG003797

da Silva Cruz, J., Blanco, C. J. C., & de Oliveira Júnior, J. F. (2022). Modeling of land use and land cover change dynamics for future projection of the Amazon number curve. *Science of the Total Environment*, *811*, 152348. https://doi.org/10.1016/j.scitotenv.2021.152348

Davidson, E. A., De Araújo, A. C., Artaxo, P., Balch, J. K., Brown, I. F., C. Bustamante, M. M., et al. (2012). The Amazon basin in transition. *Nature*, *481*(7381), 321–328. https://doi.org/10.1038/nature10717

de Melo, M. L., Kothawala, D. N., Bertilsson, S., Amaral, J. H., Forsberg, B., & Sarmento, H. (2020). Linking dissolved organic matter composition and bacterioplankton communities in an Amazon floodplain system. *Limnology & Oceanography*, *65*(1), 63–76. https://doi.org/10.1002/lno.11250

de Moraes Novo, E. M. L., de Farias Barbosa, C. C., de Freitas, R. M., Shimabukuro, Y. E., Melack, J. M., & Filho, W. P. (2006). Seasonal changes in chlorophyll distributions in Amazon floodplain lakes derived from MODIS images. *Limnology*, *7*(3), 153–161. https://doi.org/10.1007/s10201-006-0179-8

de Paiva, R. C. D., Buarque, D. C., Collischonn, W., Bonnet, M.-P., Frappart, F., Calmant, S., & Bulhões Mendes, C. A. (2013). Large-scale hydrologic and hydrodynamic modeling of the Amazon River basin. *Water Resources Research*, *49*(3), 1226–1243. https://doi.org/10.1002/wrcr.20067

Devol, A. H., Forsberg, B. R., Richey, J. E., & Pimentel, T. P. (1995). Seasonal variation in chemical distributions in the Amazon (Solimões) river: A multiyear time series. *Global Biogeochemical Cycles*, *9*(3), 307–328. https://doi.org/10.1029/95GB01145

Dittmar, T., Koch, B., Hertkorn, N., & Kattner, G. (2008). A simple and efficient method for the solid-phase extraction of dissolved organic matter (SPE-DOM) from seawater. *Limnology and Oceanography: Methods*, *6*(6), 230–235. https://doi.org/10.4319/lom.2008.6.230

Doherty, M., Yager, P. L., Moran, M. A., Coles, V. J., Fortunato, C. S., Krusche, A. V., et al. (2017). Bacterial biogeography across the Amazon River-ocean continuum. *Frontiers in Microbiology*, *8*, 882. https://doi.org/10.3389/fmicb.2017.00882

Dornblaser, M. M., & Striegl, R. G. (2009). Suspended sediment and carbonate transport in the Yukon River Basin, Alaska: Fluxes and potential future responses to climate change. *Water Resources Research*, *45*(6), 2008WR007546. https://doi.org/10.1029/2008WR007546

Drake, T. W., Hemingway, J. D., Kurek, M. R., Peucker-Ehrenbrink, B., Brown, K. A., Holmes, R. M., et al. (2021). The pulse of the Amazon: Fluxes of dissolved organic carbon, nutrients, and ions from the World's Largest River. *Global Biogeochemical Cycles*, *35*(4), e2020GB006895. https://doi.org/10.1029/2020GB006895

Drake, T. W., Raymond, P. A., & Spencer, R. G. M. (2018). Terrestrial carbon inputs to inland waters: A current synthesis of estimates and uncertainty. *Limnology and Oceanography Letters*, *3*(3), 132–142. https://doi.org/10.1002/lol2.10055

Espinoza, J.-C., Marengo, J. A., Schongart, J., & Jimenez, J. C. (2022). The new historical flood of 2021 in the Amazon River compared to major floods of the 21st century: Atmospheric features in the context of the intensification of floods. *Weather and Climate Extremes*, *35*, 100406. https://doi.org/10.1016/j.wace.2021.100406

Farella, N., Lucotte, M., Louchouarn, P., & Roulet, M. (2001). Deforestation modifying terrestrial organic transport in the Rio Tapajós, Brazilian Amazon. *Organic Geochemistry*, *32*(12), 1443–1458. https://doi.org/10.1016/S0146-6380(01)00103-6

Farinosi, F., Arias, M. E., Lee, E., Longo, M., Pereira, F. F., Livino, A., et al. (2019). Future climate and land use change impacts on river flows in the Tapajós basin in the Brazilian Amazon. *Earth's Future*, *7*(8), 993–1017. https://doi.org/10.1029/2019EF001198

Fearnside, P. M. (2018). Brazil's Amazonian forest carbon: The key to Southern Amazonia's significance for global climate. *Regional Environmental Change*, *18*(1), 47–61. https://doi.org/10.1007/s10113-016-1007-2

Friedl, M., & Sulla-Menashe, D. (2019). MCD12Q1 MODIS/Terra+Aqua land cover type yearly L3 global 500m SIN grid V006 [Dataset]. *NASA EOSDIS Land Processes Distributed Active Archive Center*. https://doi.org/10.5067/MODIS/MCD12Q1.006

Gelaro, R., McCarty, W., Suárez, M. J., Todling, R., Molod, A., Takacs, L., et al. (2017). The modern-era retrospective analysis for research and applications, version 2 (MERRA-2). *Journal of Climate*, *30*(14), 5419–5454. https://doi.org/10.1175/JCLI-D-16-0758.1

Gloor, M., Brienen, R. J. W., Galbraith, D., Feldpausch, T. R., Schöngart, J., Guyot, J.-L., et al. (2013). Intensification of the Amazon hydrological cycle over the last two decades. *Geophysical Research Letters*, *40*(9), 1729–1733. https://doi.org/10.1002/grl.50377

Gonsior, M., Valle, J., Schmitt-Kopplin, P., Hertkorn, N., Bastviken, D., Luek, J., et al. (2016). Chemodiversity of dissolved organic matter in the Amazon Basin. *Biogeosciences*, *13*(14), 4279–4290. https://doi.org/10.5194/bg-13-4279-2016

Gudmundsson, L., Boulange, J., Do, H. X., Gosling, S. N., Grillakis, M. G., Koutroulis, A. G., et al. (2021). Globally observed trends in mean and extreme river flow attributed to climate change. *Science*, *371*(6534), 1159–1162. https://doi.org/10.1126/science.aba3996

Guillemette, F., McCallister, S. L., & Del Giorgio, P. A. (2013). Differentiating the degradation dynamics of algal and terrestrial carbon within complex natural dissolved organic carbon in temperate lakes. *Journal of Geophysical Research: Biogeosciences*, *118*(3), 963–973. https://doi.org/10.1002/jgrg.20077

Guinoiseau, D., Bouchez, J., Gélabert, A., Louvat, P., Filizola, N., & Benedetti, M. F. (2016). The geochemical filter of large river confluences. *Chemical Geology*, *441*, 191–203. https://doi.org/10.1016/j.chemgeo.2016.08.009

Hastie, A., Lauerwald, R., Ciais, P., & Regnier, P. (2019). Aquatic carbon fluxes dampen the overall variation of net ecosystem productivity in the Amazon basin: An analysis of the interannual variability in the boundless carbon cycle. *Global Change Biology*, *25*(6), 2094–2111. https://doi.org/10.1111/gcb.14620

Hedges, J. I., Keil, R. G., & Benner, R. (1997). What happens to terrestrial organic matter in the ocean? *Organic Geochemistry*, *27*(5), 195–212. https://doi.org/10.1016/S0146-6380(97)00066-1

Helms, J. R., Stubbins, A., Ritchie, J. D., Minor, E. C., Kieber, D. J., & Mopper, K. (2008). Absorption spectral slopes and slope ratios as indicators of molecular weight, source, and photobleaching of chromophoric dissolved organic matter. *Limnology & Oceanography*, *53*(3), 955–969. https://doi.org/10.4319/lo.2008.53.3.0955

Hendrickson, C. L., Quinn, J. P., Kaiser, N. K., Smith, D. F., Blakney, G. T., Chen, T., et al. (2015). 21 Tesla Fourier transform ion cyclotron resonance mass spectrometer: A national resource for ultrahigh resolution mass analysis. *Journal of the American Society for Mass Spectrometry*, *26*(9), 1626–1632. https://doi.org/10.1007/s13361-015-1182-2

Hertkorn, N., Harir, M., Cawley, K. M., Schmitt-Kopplin, P., & Jaffé, R. (2016). Molecular characterization of dissolved organic matter from subtropical wetlands: A comparative study through the analysis of optical properties, NMR and FTICR/MS. *Biogeosciences*, *13*(8), 2257–2277. https://doi.org/10.5194/bg-13-2257-2016

Huffman, G. J., STocker, E. F., Bolvin, D. T., Nelkin, E. J., & Tan, J. (2019). GPM IMERG late precipitation L3 1 day 0.1 degree x 0.1 degree V06 [Dataset]. *NASA Goddard Earth Sciences Data and Information Services Center*. https://doi.org/10.5067/GPM/IMERGDL/DAY/06

Jiménez-Muñoz, J. C., Mattar, C., Barichivich, J., Santamaría-Artigas, A., Takahashi, K., Malhi, Y., et al. (2016). Record-breaking warming and extreme drought in the Amazon rainforest during the course of El Niño 2015–2016. *Scientific Reports*, *6*(1), 33130. https://doi.org/10.1038/srep33130

Junk, W. J., Piedade, M. T. F., Schöngart, J., Cohn-Haft, M., Adeney, J. M., & Wittmann, F. (2011). A classification of major naturally-occurring Amazonian lowland wetlands. *Wetlands*, *31*(4), 623–640. https://doi.org/10.1007/s13157-011-0190-7

Kellerman, A. M., Guillemette, F., Podgorski, D. C., Aiken, G. R., Butler, K. D., & Spencer, R. G. M. (2018). Unifying concepts linking dissolved organic matter composition to persistence in aquatic ecosystems. *Environmental Science & Technology*, *52*(5), 2538–2548. https://doi.org/10.1021/acs.est.7b05513

Koch, B. P., & Dittmar, T. (2006). From mass to structure: An aromaticity index for high-resolution mass data of natural organic matter. *Rapid Communications in Mass Spectrometry*, *20*(5), 926–932. https://doi.org/10.1002/rcm.2386

Koch, B. P., & Dittmar, T. (2016). From mass to structure: An aromaticity index for high-resolution mass data of natural organic matter. *Rapid Communications in Mass Spectrometry*, *30*(1), 250. https://doi.org/10.1002/rcm.7433

Kothawala, D. N., Murphy, K. R., Stedmon, C. A., Weyhenmeyer, G. A., & Tranvik, L. J. (2013). Inner filter correction of dissolved organic matter fluorescence. *Limnology and Oceanography: Methods*, *11*(12), 616–630. https://doi.org/10.4319/lom.2013.11.616

Kurek, M. (2025). Long-term and seasonal drivers of organic matter in the clearwater Tapajós River and implications for the Amazon River basin [Dataset]. *OSF*. https://doi.org/10.17605/OSF.IO/USH6Y

Kurek, M. R., Poulin, B. A., McKenna, A. M., & Spencer, R. G. M. (2020). Deciphering dissolved organic matter: Ionization, dopant, and fragmentation insights via fourier transform-ion cyclotron resonance mass spectrometry. *Environmental Science & Technology*, *54*(24), 16249–16259. https://doi.org/10.1021/acs.est.0c05206

Kurek, M. R., Stubbins, A., Drake, T. W., Dittmar, T. M. S., Moura, J., Holmes, R. M., et al. (2022). Organic molecular signatures of the Congo River and comparison to the Amazon. *Global Biogeochemical Cycles*, *36*(6), e2022GB007301. https://doi.org/10.1029/2022GB007301

Kurek, M. R., Stubbins, A., Drake, T. W., Moura, J. M. S., Holmes, R. M., Osterholz, H., et al. (2021). Drivers of organic molecular signatures in the Amazon River. *Global Biogeochemical Cycles*, *35*(6), e2021GB006938. https://doi.org/10.1029/2021GB006938

Kurek, M. R., Wickland, K. P., Nichols, N. A., McKenna, A. M., Anderson, S. M., Dornblaser, M. M., et al. (2024). Linking dissolved organic matter composition to landscape properties in wetlands across the United States of America. *Global Biogeochemical Cycles*, *38*(5), e2023GB007917. https://doi.org/10.1029/2023GB007917

Lambert, T., Bouillon, S., Darchambeau, F., Massicotte, P., & Borges, A. V. (2016). Shift in the chemical composition of dissolved organic matter in the CongoRiver network. *Biogeosciences*, *13*(18), 5405–5420. https://doi.org/10.5194/bg-13-5405-2016

Lapierre, J.-F., & Del Giorgio, P. A. (2014). Partial coupling and differential regulation of biologically and photochemically labile dissolved organic carbon across boreal aquatic networks. *Biogeosciences*, *11*(20), 5969–5985. https://doi.org/10.5194/bg-11-5969-2014

Lechtenfeld, O. J., Kattner, G., Flerus, R., McCallister, S. L., Schmitt-Kopplin, P., & Koch, B. P. (2014). Molecular transformation and degradation of refractory dissolved organic matter in the Atlantic and Southern Ocean. *Geochimica et Cosmochimica Acta*, *126*, 321–337. https://doi.org/10.1016/j.gca.2013.11.009

Li, M., Peng, C., Zhou, X., Yang, Y., Guo, Y., Shi, G., & Zhu, Q. (2019). Modeling global riverine DOC flux dynamics from 1951 to 2015. *Journal of Advances in Modeling Earth Systems*, *11*(2), 514–530. https://doi.org/10.1029/2018MS001363

Li, S., Harir, M., Schmitt-Kopplin, P., Gonsior, M., Enrich-Prast, A., Bastviken, D., et al. (2023). Comprehensive assessment of dissolved organic matter processing in the Amazon River and its major tributaries revealed by positive and negative electrospray mass spectrometry and NMR spectroscopy. *Science of the Total Environment*, *857*, 159620. https://doi.org/10.1016/j.scitotenv.2022.159620

Li, S., Harir, M., Schmitt-Kopplin, P., Machado-Silva, F., Gonsior, M., Bastviken, D., et al. (2023). Distinct non-conservative behavior of dissolved organic matter after mixing Solimões/Negro and Amazon/Tapajós River waters. *ACS ES&T Water*, *3*(8), 2083–2095. https://doi.org/10.1021/acsestwater.2c00621

Liang, Y.-C., Lo, M.-H., Lan, C.-W., Seo, H., Ummenhofer, C. C., Yeager, S., et al. (2020). Amplified seasonal cycle in hydroclimate over the Amazon river basin and its plume region. *Nature Communications*, *11*(1), 4390. https://doi.org/10.1038/s41467-020-18187-0

Lobo, F. D. L., Costa, M., de Novo, E. M. L. M., & Telmer, K. (2016). Distribution of artisanal and small-scale gold mining in the Tapajós River Basin (Brazilian Amazon) over the past 40 Years and relationship with water siltation. *Remote Sensing*, *8*(7), 579. Article 7. https://doi.org/10.3390/rs8070579

Lobo, F. D. L., Costa, M., Novo, E. M. L. D. M., & Telmer, K. (2017). Effects of small-scale gold mining tailings on the underwater light field in the Tapajós River Basin, Brazilian Amazon. *Remote Sensing*, *9*(8), 861. Article 8. https://doi.org/10.3390/rs9080861

Mann, P. J., Spencer, R. G. M., Dinga, B. J., Poulsen, J. R., Hernes, P. J., Fiske, G., et al. (2014). The biogeochemistry of carbon across a gradient of streams and rivers within the Congo Basin: Aquatic C biogeochemistry in Congo Basin. *Journal of Geophysical Research: Biogeosciences*, *119*(4), 687–702. https://doi.org/10.1002/2013JG002442

Marengo, J. A. (2006). On the hydrological cycle of the Amazon basin: A historical review and current state-of-the-art. *Revista Brasileira de Meteorologia*, *21*, 1–19.

Martinelli, L. A., Victoria, R. L., Silveira Lobo Sternberg, L., Ribeiro, A., & Zacharias Moreira, M. (1996). Using stable isotopes to determine sources of evaporated water to the atmosphere in the Amazon basin. *Journal of Hydrology*, *183*(3), 191–204. https://doi.org/10.1016/0022-1694(95)02974-5

Mayorga, E., Aufdenkampe, A. K., Masiello, C. A., Krusche, A. V., Hedges, J. I., Quay, P. D., et al. (2005). Young organic matter as a source of carbon dioxide outgassing from Amazonian rivers. *Nature*, *436*(7050), 538–541. https://doi.org/10.1038/nature03880

McClain, M. E., Richey, J. E., Brandes, J. A., & Pimentel, T. P. (1997). Dissolved organic matter and terrestrial-lotic linkages in the Central Amazon Basin of Brazil. *Global Biogeochemical Cycles*, *11*(3), 295–311. https://doi.org/10.1029/97GB01056

McDonough, L. K., Andersen, M. S., Behnke, M. I., Rutlidge, H., Oudone, P., Meredith, K., et al. (2022). A new conceptual framework for the transformation of groundwater dissolved organic matter. *Nature Communications*, *13*(1), 2153. https://doi.org/10.1038/s41467-022-29711-9

McKnight, D. M., Boyer, E. W., Westerhoff, P. K., Doran, P. T., Kulbe, T., & Andersen, D. T. (2001). Spectrofluorometric characterization of dissolved organic matter for indication of precursor organic material and aromaticity. *Limnology & Oceanography*, *46*(1), 38–48. https://doi.org/10.4319/lo.2001.46.1.0038

Medeiros, P. M., Seidel, M., Ward, N. D., Carpenter, E. J., Gomes, H. R., Niggemann, J., et al. (2015). Fate of the Amazon River dissolved organic matter in the tropical Atlantic Ocean. *Global Biogeochemical Cycles*, *29*(5), 677–690. https://doi.org/10.1002/2015GB005115

Moquet, J.-S., Guyot, J.-L., Crave, A., Viers, J., Filizola, N., Martinez, J.-M., et al. (2016). Amazon River dissolved load: Temporal dynamics and annual budget from the Andes to the ocean. *Environmental Science and Pollution Research*, *23*(12), 11405–11429. https://doi.org/10.1007/s11356-015-5503-6

Moreira-Turcq, P., Seyler, P., Guyot, J. L., & Etcheber, H. (2003). Exportation of organic carbon from the Amazon River and its main tributaries. *Hydrological Processes*, *17*(7), 1329–1344. https://doi.org/10.1002/hyp.1287

Mortatti, J., Moraes, J. M., Victoria, R. L., & Martinelli, L. A. (1997). Hydrograph separation of the Amazon River: A methodological study. *Aquatic Geochemistry*, *3*(2), 117–128. https://doi.org/10.1023/A:1009606801595

Murphy, K. R., Stedmon, C. A., Graeber, D., & Bro, R. (2013). Fluorescence spectroscopy and multi-way techniques. PARAFAC. *Analytical Methods*, *5*(23), 6557. https://doi.org/10.1039/c3ay41160e

Musolff, A., Schmidt, C., Selle, B., & Fleckenstein, J. H. (2015). Catchment controls on solute export. *Advances in Water Resources*, *86*, 133–146. https://doi.org/10.1016/j.advwatres.2015.09.026

Neu, V., Da, S., Araújo, M. G., Guedes, V. M., Ward, N. D., Ribeiro, M. M., et al. (2023). Composition and flux of dissolved and particulate carbon and nitrogen in the lower Tocantins River. *Journal of Geophysical Research: Biogeosciences*, *128*(6), e2022JG006846. https://doi.org/10.1029/2022JG006846

Nóbrega, R. L. B., Guzha, A. C., Lamparter, G., Amorim, R. S. S., Couto, E. G., Hughes, H. J., et al. (2018). Impacts of land-use and land-cover change on stream hydrochemistry in the Cerrado and Amazon biomes. *Science of the Total Environment*, *635*, 259–274. https://doi.org/10.1016/j.scitotenv.2018.03.356

Nóbrega, R. L. B., Lamparter, G., Hughes, H., Guzha, A. C., Amorim, R. S. S., & Gerold, G. (2018). A multi-approach and multi-scale study on water quantity and quality changes in the Tapajós River basin, Amazon. *Proceedings of the International Association of Hydrological Sciences*, *377*, 3–7. https://doi.org/10.5194/piahs-377-3-2018

Osterholz, H., Kirchman, D. L., Niggemann, J., & Dittmar, T. (2016). Environmental drivers of dissolved organic matter molecular composition in the Delaware estuary. *Frontiers in Earth Science*, *4*. https://doi.org/10.3389/feart.2016.00095

Panday, P. K., Coe, M. T., Macedo, M. N., Lefebvre, P., & de Castanho, A. D. A. (2015). Deforestation offsets water balance changes due to climate variability in the Xingu River in eastern Amazonia. *Journal of Hydrology*, *523*, 822–829. https://doi.org/10.1016/j.jhydrol.2015.02.018

Patriarca, C., Sedano-Núñez, V. T., Garcia, S. L., Bergquist, J., Bertilsson, S., Sjöberg, P. J. R., et al. (2021). Character and environmental lability of cyanobacteria-derived dissolved organic matter. *Limnology & Oceanography*, *66*(2), 496–509. https://doi.org/10.1002/lno.11619

Pavanato, H., Melo-Santos, G., Lima, D., Portocarrero-Aya, M., Paschoalini, M., Mosquera, F., et al. (2016). Risks of dam construction for south American River dolphins: A case study of the Tapajós River. *Endangered Species Research*, *31*, 47–60. https://doi.org/10.3354/esr00751

Poulin, B. A., Ryan, J. N., Nagy, K. L., Stubbins, A., Dittmar, T., Orem, W., et al. (2017). Spatial dependence of reduced sulfur in everglades dissolved organic matter controlled by sulfate enrichment. *Environmental Science & Technology*, *51*(7), 3630–3639. https://doi.org/10.1021/acs.est.6b04142

Qu, L., Wu, Y., Li, Y., Stubbins, A., Dahlgren, R. A., Chen, N., & Guo, W. (2020). El Niño-driven dry season flushing enhances dissolved organic matter export from a subtropical watershed. *Geophysical Research Letters*, *47*(19), e2020GL089877. https://doi.org/10.1029/2020GL089877

Quay, P. D., Wilbur, D., Richey, J. E., Hedges, J. I., Devol, A. H., & Victoria, R. (1992). Carbon cycling in the Amazon River: Implications from the 13C compositions of particles and solutes. *Limnology & Oceanography*, *37*(4), 857–871. https://doi.org/10.4319/lo.1992.37.4.0857

Raymond, P. A., Hartmann, J., Lauerwald, R., Sobek, S., McDonald, C., Hoover, M., et al. (2013). Global carbon dioxide emissions from inland waters. *Nature*, *503*(7476), 355–359. https://doi.org/10.1038/nature12760

Raymond, P. A., Saiers, J. E., & Sobczak, W. V. (2016). Hydrological and biogeochemical controls on watershed dissolved organic matter transport: Pulse-shunt concept. *Ecology*, *97*(1), 5–16. https://doi.org/10.1890/14-1684.1

R Core Team. (2020). R: A language and environment for statistical computing. *The R Project for Statistical Computing*. Retrieved from https://www.r-project.org/

Revelle, W. (2024). psych: Procedures for psychological, psychometric, and personality Research (version 2.4.6.26) [Computer Software]. https://cran.r-project.org/web/packages/psych/index.html

Richey, J. E., Hedges, J. I., Devol, A. H., Quay, P. D., Victoria, R., Martinelli, L., & Forsberg, B. R. (1990). Biogeochemistry of carbon in the Amazon River. *Limnology & Oceanography*, *35*(2), 352–371. https://doi.org/10.4319/lo.1990.35.2.0352

Richey, J. E., Mertes, L. A. K., Dunne, T., Victoria, R. L., Forsberg, B. R., Tancredi, A. C. N. S., & Oliveira, E. (1989). Sources and routing of the Amazon River flood wave. *Global Biogeochemical Cycles*, *3*(3), 191–204. https://doi.org/10.1029/GB003i003p00191

Riedel, T., Zark, M., Vähätalo, A. V., Niggemann, J., Spencer, R. G. M., Hernes, P. J., & Dittmar, T. (2016). Molecular signatures of biogeochemical transformations in dissolved organic matter from ten world rivers. *Frontiers in Earth Science*, *4*. https://doi.org/10.3389/feart.2016.00085

Ríos-Villamizar, E. A., Adeney, J. M., Piedade, M. T. F., & Junk, W. J. (2020). New insights on the classification of major Amazonian river water types. *Sustainable Water Resources Management*, *6*(5), 83. https://doi.org/10.1007/s40899-020-00440-5

Rose, L. A., Karwan, D. L., & Godsey, S. E. (2018). Concentration–discharge relationships describe solute and sediment mobilization, reaction, and transport at event and longer timescales. *Hydrological Processes*, *32*(18), 2829–2844. https://doi.org/10.1002/hyp.13235

Rosengard, S. Z., Moura, J. M. S., Spencer, R. G. M., Johnson, C., McNichol, A., Steen, A. D., & Galy, V. (2024). Depth-partitioning of particulate organic carbon composition in the rising and falling stages of the Amazon River. *Geochemistry, Geophysics, Geosystems*, *25*(6), e2023GC011273. https://doi.org/10.1029/2023GC011273

Runkel, R. L., Crawford, C. G., & Cohn, T. A. (2004). Load estimator (LOADEST): A FORTRAN program for estimating constituent loads in streams and rivers. *Techniques and Methods*. Article 4-A5. https://doi.org/10.3133/tm4A5

Salati, E., Dall'Olio, A., Matsui, E., & Gat, J. R. (1979). Recycling of water in the Amazon Basin: An isotopic study. *Water Resources Research*, *15*(5), 1250–1258. https://doi.org/10.1029/WR015i005p01250

Šantl-Temkiv, T., Finster, K., Dittmar, T., Hansen, B. M., Thyrhaug, R., Nielsen, N. W., & Karlson, U. G. (2013). Hailstones: A window into the microbial and chemical inventory of a storm cloud. *PLoS One*, *8*(1), e53550. https://doi.org/10.1371/journal.pone.0053550

Savory, J. J., Kaiser, N. K., McKenna, A. M., Xian, F., Blakney, G. T., Rodgers, R. P., et al. (2011). Parts-per-billion fourier transform ion cyclotron resonance mass measurement accuracy with a "Walking" calibration equation. *Analytical Chemistry*, *83*(5), 1732–1736. https://doi.org/10.1021/ac102943z

Sawakuchi, H. O., Bastviken, D., Sawakuchi, A. O., Krusche, A. V., Ballester, M. V. R., & Richey, J. E. (2014). Methane emissions from Amazonian Rivers and their contribution to the global methane budget. *Global Change Biology*, *20*(9), 2829–2840. https://doi.org/10.1111/gcb.12646

Sawakuchi, H. O., Neu, V., Ward, N. D., Barros, M. D. L. C., Valerio, A. M., Gagne-Maynard, W., et al. (2017). Carbon dioxide emissions along the lower Amazon River. *Frontiers in Marine Science*, *4*, 76. https://doi.org/10.3389/fmars.2017.00076

Seidel, M., Dittmar, T., Ward, N. D., Krusche, A. V., Richey, J. E., Yager, P. L., & Medeiros, P. M. (2016). Seasonal and spatial variability of dissolved organic matter composition in the lower Amazon River. *Biogeochemistry*, *131*(3), 281–302. https://doi.org/10.1007/s10533-016-0279-4

Seidel, M., Yager, P. L., Ward, N. D., Carpenter, E. J., Gomes, H. R., Krusche, A. V., et al. (2015). Molecular-level changes of dissolved organic matter along the Amazon River-to-ocean continuum. *Marine Chemistry*, *177*, 218–231. https://doi.org/10.1016/j.marchem.2015.06.019

Seifert, A.-G., Roth, V.-N., Dittmar, T., Gleixner, G., Breuer, L., Houska, T., & Marxsen, J. (2016). Comparing molecular composition of dissolved organic matter in soil and stream water: Influence of land use and chemical characteristics. *Science of the Total Environment*, *571*, 142–152. https://doi.org/10.1016/j.scitotenv.2016.07.033

Seyler, P., Coynel, A., Moreira-Turcq, P., Etcheber, H., Colas, C., Orange, D., et al. (2005). Organic carbon transported by the equatorial rivers: Example of Congo-Zaire and Amazon basins. In *Soil erosion and carbon dynamics*. CRC Press.

Simon, C., Osterholz, H., Koschinsky, A., & Dittmar, T. (2019). Riverine mixing at the molecular scale – An ultrahigh-resolution mass spectrometry study on dissolved organic matter and selected metals in the Amazon confluence zone (Manaus, Brazil). *Organic Geochemistry*, *129*, 45–62. https://doi.org/10.1016/j.orggeochem.2019.01.013

Simon, C., Pimentel, T. P., Monteiro, M. T. F., Candido, L. A., Gastmans, D., Geilmann, H., et al. (2021). Molecular links between whitesand ecosystems and blackwater formation in the Rio Negro watershed. *Geochimica et Cosmochimica Acta*, *311*, 274–291. https://doi.org/10.1016/j.gca.2021.06.036

Sioli, H. (Ed.). (1984). *The Amazon: Limnology and landscape ecology of a mighty tropical river and its basin* (Vol. 56). Springer. https://doi.org/10.1007/978-94-009-6542-3

Smith, D. F., Podgorski, D. C., Rodgers, R. P., Blakney, G. T., & Hendrickson, C. L. (2018). 21 Tesla FT-ICR mass spectrometer for ultrahigh-resolution analysis of complex organic mixtures. *Analytical Chemistry*, *90*(3), 2041–2047. https://doi.org/10.1021/acs.analchem.7b04159

Souza, T., Araujo, D. J., Cassimiro, C. A. L., & Batista, D. S. (2024). Chemodiversity of dissolved soil organic matter from Amazon rainforest as influenced by deforestation. *Metabolites*, *14*(3), 144. https://doi.org/10.3390/metabo14030144

Spencer, R. G., Hernes, P. J., Ruf, R., Baker, A., Dyda, R. Y., Stubbins, A., & Six, J. (2010). Temporal controls on dissolved organic matter and lignin biogeochemistry in a pristine tropical river, Democratic Republic of Congo. *Journal of Geophysical Research: Biogeosciences*, *115*(G3). https://doi.org/10.1029/2009JG001180

Spencer, R. G. M., Butler, K. D., & Aiken, G. R. (2012). Dissolved organic carbon and chromophoric dissolved organic matter properties of rivers in the USA. *Journal of Geophysical Research: Biogeosciences*, *117*(G3), 2011JG001928. https://doi.org/10.1029/2011JG001928

Spencer, R. G. M., Kellerman, A. M., Podgorski, D. C., Macedo, M. N., Jankowski, K., Nunes, D., & Neill, C. (2019). Identifying the molecular signatures of agricultural expansion in Amazonian headwater streams. *Journal of Geophysical Research: Biogeosciences*, *124*(6), 1637–1650. https://doi.org/10.1029/2018JG004910

Spencer, R. G. M., & Raymond, P. A. (2024). Chapter 14—Riverine DOM. In D. A. Hansell & C. A. Carlson (Eds.), *Biogeochemistry of marine dissolved organic matter* (3rd ed., pp. 657–691). Academic Press. https://doi.org/10.1016/B978-0-443-13858-4.00014-9

Stedmon, C. A., Markager, S., & Bro, R. (2003). Tracing dissolved organic matter in aquatic environments using a new approach to fluorescence spectroscopy. *Marine Chemistry*, *82*(3), 239–254. https://doi.org/10.1016/S0304-4203(03)00072-0

Tardy, Y., Bustillo, V., Roquin, C., Mortatti, J., & Victoria, R. (2005). The Amazon. Bio-Geochemistry applied to river basin management: Part I. Hydro-Climatology, hydrograph separation, mass transfer balances, stable isotopes, and modelling. *Applied Geochemistry*, *20*(9), 1746–1829. https://doi.org/10.1016/j.apgeochem.2005.06.001

Textor, S. R., Guillemette, F., Zito, P. A., & Spencer, R. G. M. (2018). An assessment of dissolved organic carbon biodegradability and priming in blackwater systems. *Journal of Geophysical Research: Biogeosciences*, *123*(9), 2998–3015. https://doi.org/10.1029/2018JG004470

Torres, K. M. A., Lopes, R. B., Passos, C. J. S., Pereira, A. C., & de Moura, L. S. (2020). Dominance of potentially toxic cyanobacteria on the waterfront of Santarém, Tapajós River, Brazilian Amazon. *Revista Ibero-Americana de Ciências Ambientais*, *11*(6), 298–314. Article 6. https://doi.org/10.6008/CBPC2179-6858.2020.006.0025

Vannote, R. L., Minshall, G. W., Cummins, K. W., Sedell, J. R., & Cushing, C. E. (1980). The River continuum concept. *Canadian Journal of Fisheries and Aquatic Sciences*, *37*(1), 130–137. https://doi.org/10.1139/f80-017

Van Schaik, E., Killaars, L., Smith, N. E., Koren, G., Van Beek, L. P. H., Peters, W., & Van Der Laan-Luijkx, I. T. (2018). Changes in surface hydrology, soil moisture and gross primary production in the Amazon during the 2015/2016 El Niño. *Philosophical Transactions of the Royal Society B: Biological Sciences*, *373*(1760), 20180084. https://doi.org/10.1098/rstb.2018.0084

Van Vliet, M. T. H., Franssen, W. H. P., Yearsley, J. R., Ludwig, F., Haddeland, I., Lettenmaier, D. P., & Kabat, P. (2013). Global river discharge and water temperature under climate change. *Global Environmental Change*, *23*(2), 450–464. https://doi.org/10.1016/j.gloenvcha.2012.11.002

Wagner, S., Fair, J. H., Matt, S., Hosen, J. D., Raymond, P., Saiers, J., et al. (2019). Molecular hysteresis: Hydrologically driven changes in riverine dissolved organic matter Chemistry during a storm event. *Journal of Geophysical Research: Biogeosciences*, *124*(4), 759–774. https://doi.org/10.1029/2018JG004817

Wagner, S., Riedel, T., Niggemann, J., Vähätalo, A. V., Dittmar, T., & Jaffé, R. (2015). Linking the molecular signature of heteroatomic dissolved organic matter to watershed characteristics in world rivers. *Environmental Science & Technology*, *49*(23), 13798–13806. https://doi.org/10.1021/acs.est.5b00525

Ward, N. D., Bianchi, T. S., Sawakuchi, H. O., Gagne-Maynard, W., Cunha, A. C., Brito, D. C., et al. (2016). The reactivity of plant-derived organic matter and the potential importance of priming effects along the lower Amazon River. *Journal of Geophysical Research: Biogeosciences*, *121*(6), 1522–1539. https://doi.org/10.1002/2016JG003342

Ward, N. D., Keil, R. G., Medeiros, P. M., Brito, D. C., Cunha, A. C., Dittmar, T., et al. (2013). Degradation of terrestrially derived macromolecules in the Amazon River. *Nature Geoscience*, *6*(7), 530–533. https://doi.org/10.1038/ngeo1817

Ward, N. D., Krusche, A. V., Sawakuchi, H. O., Brito, D. C., Cunha, A. C., Moura, J. M. S., et al. (2015). The compositional evolution of dissolved and particulate organic matter along the lower Amazon River—Óbidos to the ocean. *Marine Chemistry*, *177*, 244–256. https://doi.org/10.1016/j.marchem.2015.06.013

Weishaar, J. L., Aiken, G. R., Bergamaschi, B. A., Fram, M. S., Fujii, R., & Mopper, K. (2003). Evaluation of specific ultraviolet absorbance as an indicator of the chemical composition and reactivity of dissolved organic carbon. *Environmental Science & Technology*, *37*(20), 4702–4708. https://doi.org/10.1021/es030360x

Wickham, H. (2016). *ggplot2: Elegant graphics for data analysis* (2nd ed. 2016). Springer International Publishing. https://doi.org/10.1007/978-3-319-24277-4

WISER. (2022). IAEA water isotope system for electronic retrieval [Dataset]. Retrieved from https://nucleus.iaea.org/wiser

Wu, Q., Ke, L., Wang, J., Pavelsky, T. M., Allen, G. H., Sheng, Y., et al. (2023). Satellites reveal hotspots of global river extent change. *Nature Communications*, *14*(1), 1587. https://doi.org/10.1038/s41467-023-37061-3

Xian, F., Hendrickson, C. L., Blakney, G. T., Beu, S. C., & Marshall, A. G. (2010). Automated broadband phase correction of fourier transform ion cyclotron resonance mass spectra. *Analytical Chemistry*, *82*(21), 8807–8812. https://doi.org/10.1021/ac101091w

Yvin, O. M., Kurek, M. R., McKenna, A. M., Hawkings, J. R., & Spencer, R. G. M. (2024). Comparison of dissolved organic matter composition from various sorbents using ultra-high resolution mass spectrometry. *Organic Geochemistry*, *196*, 104846. https://doi.org/10.1016/j.orggeochem.2024.104846

Zhang, F., Harir, M., Moritz, F., Zhang, J., Witting, M., Wu, Y., et al. (2014). Molecular and structural characterization of dissolved organic matter during and post cyanobacterial bloom in Taihu by combination of NMR spectroscopy and FTICR mass spectrometry. *Water Research*, *57*, 280–294. https://doi.org/10.1016/j.watres.2014.02.051

References From the Supporting Information

Andersson, M. G. I., Catalán, N., Rahman, Z., Tranvik, L. J., & Lindström, E. S. (2018). Effects of sterilization on dissolved organic carbon (DOC) composition and bacterial utilization of DOC from lakes. *Aquatic Microbial Ecology*, *82*(2), 199–208. https://doi.org/10.3354/ame01890

Bittar, T. B., Berger, S. A., Birsa, L. M., Walters, T. L., Thompson, M. E., Spencer, R. G. M., et al. (2016). Seasonal dynamics of dissolved, particulate and microbial components of a tidal saltmarsh-dominated estuary under contrasting levels of freshwater discharge. *Estuarine, Coastal and Shelf Science*, *182*, 72–85. https://doi.org/10.1016/j.ecss.2016.08.046

Blakney, G. T., Hendrickson, C. L., & Marshall, A. G. (2011). Predator data station: A fast data acquisition system for advanced FT-ICR MS experiments. *International Journal of Mass Spectrometry*, *306*(2), 246–252. https://doi.org/10.1016/j.ijms.2011.03.009

Boldin, I. A., & Nikolaev, E. N. (2011). Fourier transform ion cyclotron resonance cell with dynamic harmonization of the electric field in the whole volume by shaping of the excitation and detection electrode assembly. *Rapid Communications in Mass Spectrometry*, *25*(1), 122–126. https://doi.org/10.1002/rcm.4838

Chen, T., Beu, S. C., Kaiser, N. K., & Hendrickson, C. L. (2014). Note: Optimized circuit for excitation and detection with one pair of electrodes for improved Fourier transform ion cyclotron resonance mass spectrometry. *Review of Scientific Instruments*, *85*(6), 066107. https://doi.org/10.1063/1.4883179

da Cruz, J. S., Blanco, C. J. C., & Junior, A. C. P. B. (2020). Flow-velocity model for hydrokinetic energy availability assessment in the Amazon. *Acta Scientiarum. Technology*, *42*. Retrieved from https://www.redalyc.org/journal/3032/303265671025/html/

Derrien, M., Kim, M.-S., Ock, G., Hong, S., Cho, J., Shin, K.-H., & Hur, J. (2018). Estimation of different source contributions to sediment organic matter in an agricultural-forested watershed using end member mixing analyses based on stable isotope ratios and fluorescence spectroscopy. *Science of the Total Environment*, *618*, 569–578. https://doi.org/10.1016/j.scitotenv.2017.11.067

Hughey, C. A., Hendrickson, C. L., Rodgers, R. P., Marshall, A. G., & Qian, K. (2001). Kendrick mass defect spectrum: A compact visual analysis for ultrahigh-resolution broadband mass spectra. *Analytical Chemistry*, *73*(19), 4676–4681. https://doi.org/10.1021/ac010560w

Kaiser, N. K., McKenna, A. M., Savory, J. J., Hendrickson, C. L., & Marshall, A. G. (2013). Tailored ion radius distribution for increased dynamic range in FT-ICR mass analysis of complex mixtures. *Analytical Chemistry*, *85*(1), 265–272. https://doi.org/10.1021/ac302678v

Kendrick, E. (1963). A mass scale based on CH 2 = 14.0000 for high resolution mass spectrometry of organic compounds. *Analytical Chemistry*, *35*(13), 2146–2154. https://doi.org/10.1021/ac60206a048

Obrador, B., von Schiller, D., Marcé, R., Gómez-Gener, L., Koschorreck, M., Borrego, C., & Catalán, N. (2018). Dry habitats sustain high CO2 emissions from temporary ponds across seasons. *Scientific Reports*, *8*(1), 3015. https://doi.org/10.1038/s41598-018-20969-y

Shakil, S., Tank, S. E., Kokelj, S. V., Vonk, J. E., & Zolkos, S. (2020). Particulate dominance of organic carbon mobilization from thaw slumps on the Peel Plateau, NT: Quantification and implications for stream systems and permafrost carbon release. *Environmental Research Letters*, *15*(11), 114019. https://doi.org/10.1088/1748-9326/abac36

Stedmon, C. A., Seredyńska-Sobecka, B., Boe-Hansen, R., Le Tallec, N., Waul, C. K., & Arvin, E. (2011). A potential approach for monitoring drinking water quality from groundwater systems using organic matter fluorescence as an early warning for contamination events. *Water Research*, *45*(18), 6030–6038. https://doi.org/10.1016/j.watres.2011.08.066

Walker, S. A., Amon, R. M. W., Stedmon, C., Duan, S., & Louchouarn, P. (2009). The use of PARAFAC modeling to trace terrestrial dissolved organic matter and fingerprint water masses in coastal Canadian Arctic surface waters. *Journal of Geophysical Research: Biogeosciences*, *114*(G4). https://doi.org/10.1029/2009JG000990

Wheeler, K. I., Levia, D. F., & Hudson, J. E. (2017). Tracking senescence-induced patterns in leaf litter leachate using parallel factor analysis (PARAFAC) modeling and self-organizing maps. *Journal of Geophysical Research: Biogeosciences*, *122*(9), 2233–2250. https://doi.org/10.1002/2016JG003677

Wünsch, U. J., Murphy, K. R., & Stedmon, C. A. (2017). The one-sample PARAFAC approach reveals molecular size distributions of fluorescent components in dissolved organic matter. *Environmental Science & Technology*, *51*(20), 11900–11908. https://doi.org/10.1021/acs.est.7b03260

Yamashita, Y., Panton, A., Mahaffey, C., & Jaffé, R. (2011a). Assessing the spatial and temporal variability of dissolved organic matter in Liverpool Bay using excitation–emission matrix fluorescence and parallel factor analysis. *Ocean Dynamics*, *61*(5), 569–579. https://doi.org/10.1007/s10236-010-0365-4

Yamashita, Y., Kloeppel, B. D., Knoepp, J., Zausen, G. L., & Jaffé, R. (2011b). Effects of watershed history on dissolved organic matter characteristics in headwater streams. *Ecosystems*, *14*(7), 1110–1122. https://doi.org/10.1007/s10021-011-9469-z